

Isolated theta waves originating from the midline thalamus trigger memory reactivation during NREM sleep in mice

Corresponding Author: Dr Chao He

This file contains all reviewer reports in order by version, followed by all author rebuttals in order by version.

Version 0:

Reviewer comments:

Reviewer #1

(Remarks to the Author)

The neural mechanisms driving reactivation of neural ensembles during NREM sleep remain poorly understood. In introduction the author emphasized that the midline thalamic neurons display distinct characteristics compared to these wakefulness-promoting neurons. These midline thalamic neurons exhibit burst firing during NREM sleep and thus may play a crucial role in driving reactivation of neural ensembles associated with memory consolidation during NREM sleep. Combining multi-channel single-unit recording, closed-loop optogenetic intervention, chemogenetic intervention, fiber photometry recording, whole-cell patch clamp recording and other methods, this study demonstrated that the neural ensembles in the medial entorhinal cortex (MEC) that encode spatial experiences exhibit transient high frequency firing pattern during NREM sleep. These results suggest that isolated theta waves of the nucleus reuniens (RE) in the midline thalamus serve as a reliable sign of reactivation. Closed-loop optogenetic inhibition of RE-MEC pathway specifically suppressed these isolated theta waves, resulting in impaired reactivation and compromised memory consolidation following a spatial memory task. Taken together, these results reveal that the midline thalamus has a unique role in memory consolidation during NREM. Although the study offers novel perspectives on the mechanisms by which sleep enhances memory consolidation, the functional role of RE-MEC pathway is not sufficiently demonstrated with the current data and thus need further supporting evidence. Moreover, more detailed method descriptions are required as pointed below.

Major comments:

1. According to the firing pattern detected by principal component during training phase (left) and post-training phase in Fig 1E, MEC cell ensembles with highest principal component (PC) intensity and corresponding reactivation strength fired at high frequency, which were more likely to be interneurons. However, subsequent results indicated that MEC excitatory glutamatergic neurons, but not inhibitory interneurons, efficiently integrate excitatory inputs of RE at theta frequency band in vitro (Fig 3). Please explain the contradictory results. For this purpose, I suggest to distinguish inhibitory neurons and excitatory neurons of MEC in Fig 1. It will help to determine the main neural types involved in this reactivation.

2. Simultaneous analysis of EEG and EMG of this study showed that animals spent most time in NREM sleep and very little time in rapid eye movement (REM) sleep (Extended Data Fig. 1A-B, line of 108-110), therefore, the study focused only on NREM sleep in the subsequent analyses. However, numerous researches before had proved that theta waves were mostly present during REM sleep (Buzsáki, 2002; Jouvet, 1969, see references below for detail) and during various types of locomotor activities (Vanderwolf, 1969). Moreover, previous studies had even shown that theta waves were absent in the immobile animal (Bland, 1986). Considering so many opposite conclusions, the author need to explain these contradictory results anyway.

References:

Bland, B. H. (1986). The physiology and pharmacology of hippocampal formation theta rhythms. *Prog Neurobiol*, 26(1), 1-54. doi: 10.1016/0301-0082(86)90019-5

Buzsáki, G. (2002). Theta Oscillations in the Hippocampus. *Neuron*, 33(3), 325-340. doi: [https://doi.org/10.1016/S0896-6273\(02\)00586-X](https://doi.org/10.1016/S0896-6273(02)00586-X)

Jouvet, M. (1969). Biogenic amines and the states of sleep. *Science*, 163(3862), 32-41. doi: 10.1126/science.163.3862.32

Vanderwolf, C. H. (1969). Hippocampal electrical activity and voluntary movement in the rat. *Electroencephalography and Clinical Neurophysiology*, 26(4), 407-418. doi: 10.1016/0013-4694(69)90092-3

3. It's an interesting observation that the synchronized activity shifted from theta frequency band to gamma frequency band

when entering the waking state (Extended Data Fig. 3A-C). Then, will this dynamic change in oscillatory still occurred if the waking state is further subdivided into locomotor state or resting state? For example, this change occurred in both locomotor and resting state or only occurred in one of the two states?

4. In the line of 203-205 evidences were insufficient to support the results stated. More experiments and analyses were needed to prove the temporal directionality between RE and MEC in memory information transfer, such as Granger causality analysis, etc.

5. Did the MEC reactivated cell ensembles include grid cells? If yes, did the reactivation only occurred in grid cells?

6. Fig 4H: please explain the obvious difference in the baseline behavior performance of the mCherry-expression mice and hm4Di-expression mice on the first day. Will this difference affect your present findings and conclusions? Or the findings could be related to this baseline difference?

7. How long did the closed-loop optogenetic intervention totally last? How did a closed-loop optogenetic program stop when the animal was not under the NREM state? Did the author applied the closed-loop optogenetic intervention selectively under the NREM state. If not, how to rule out that the theta wave was also interfered when the animal's state changed from NREM to wakefulness? Please answer these questions in detail in both the Results and Method section.

8. Cited studies indicate that cells in the midline thalamic nuclei can generate burst-mode discharges lasting about hundreds of milliseconds during NREM sleep (in the line of 181-183). Did the author obtained any experimental evidence supporting that RE burst discharge can drive neocortical high-frequency oscillations, both in MEC and PFC?

9. Fig 3: RE neuron projections to the MEC labeled by calcium indicator GCamp7b are not selective for excitatory or inhibitory neurons. Then, it is necessary to conduct control experiments (brain region control) to better explain the strong correlation between calcium activities of projection neurons in RE and theta event power in MEC.

Minor comments:

1. The author need to restructure the sentence in line 102-104 and clearly state the time period of behavioral studies for better understanding

2. Did the abbreviation PC stand for principal components or principal cells? Please indicate clearly when it first appeared in the line of 119.

3. Please explain the rationale for statistical methods in line 130-134 and provide reliable references.

4. Fig 1E: to provide the meaning of each element in the figure in legend, including capital letters A...D and different colors. In addition, please explain clearly the relationship between firing frequency/pattern, PC intensity and reactivation strength. Moreover, the author also needs to explain why the high reactivation values can reflect that the firing pattern is a closer match to learning-related firing pattern (line of 120-122).

5. Fig 1F: the values of reactivation strength on day 1 and day 2 was about 1, but the firing pattern detected by principal component showed no reactivation cells in Fig 1E, please explain these contradictory results.

6. Fig 1G upper: both raw signals and band-passed signals (0.5-4 Hz, 4-12 Hz) should be presented, same problem of Fig 2D.

Fig 1H-I: only theta events were analyzed, please complete the analysis of delta events.

Fig 1G-I: only LFP waves during NREM were shown, no signal of awakening stage was found.

Three points above are inconsistent with the result statement in the line of 146-148- 'continuous delta waves (0.5-4 Hz) and discrete theta (4-12 Hz) events in the MEC recordings were evident during NREM sleep compared with that during the awakening stage'.

7. Fig 1I: the meaning of phrase 'Non-theta events' in the illustration is unclear. In addition, please check and correct the proportion value of theta band power and 'non-isolated theta' in the line of 151-152.

8. Extended Data Fig. 4: What's the meaning of 'integrated strength', and how to evaluate it.

9. The author needs to check the figures and legends thoroughly and complete the meaning of all elements in the figure legends.

10. Please clearly indicate the number of animals used in the corresponding legend of each statistical chart.

Reviewer #2

(Remarks to the Author)

Using a variety of cutting-edge technologies, such as single-unit electrophysiology, closed-loop optogenetics, Ca²⁺ photometry, and chemogenetics, Xiao et al. demonstrated that the medial entorhinal cortex (MEC) receives excitatory monosynaptic projections from the nucleus reuniens of the midline thalamus. Additionally, they discovered that the nucleus

reuniens drives transient delta wave-nested theta events in the MEC during NREM sleep, facilitating memory reactivation following a spatial memory task and essential for memory consolidation.

This study presents a well-controlled investigation with intriguing and pioneering findings. Notably, besides the previously documented sharp waves, ripples, and spindles, this research unveils a new type of network oscillatory dynamics that instigate memory trace replay during sleep, shedding light on the associated neural circuit mechanisms. However, some points require attention in a revision to support the interpretation of results:

1. In Figures 2F and 2H, the authors demonstrated the existence of excitatory monosynaptic connections between RE and MEC through patch clamp recording combined with optogenetic techniques. However, the electrophysiological data primarily supported the conclusion through the application of glutamate receptor blockers, which may not be sufficient. It is recommended that the authors further analyze the latency of postsynaptic responses after optogenetic activation of the axonal terminals.
2. Figure 3 presents simultaneous recordings of EEG, EMG, and calcium signals, yet the analysis only delves into the relationship between calcium peaks and MEC local field potentials during NREM sleep. Further elucidation is needed regarding the changes in neurons projected by RE to MEC during awakening and NREM sleep.
3. The authors mentioned including only animals with accurate recording sites. However, the number of excluded animals in some experiments, such as Figures 1 and 3, is not detailed. Moreover, clarity is needed on whether the same animals were used in Figures 2A-E and SI Fig. 5. Detailed information should be provided on these experiments.
4. The manuscript partially displays results in Figure 3, with vague descriptions. Clarification is needed on how the data presented in Figures 3E and 3F are standardized.
5. Some statistical graphs appear non-uniformly presented, notably in Figure 5, differing from others. The authors should describe the statistical charts used and explain the rationale behind the varied presentation.

Minor:

Figures 3 and Extended Data Fig. 6 depict optical fiber diagrams inconsistently. It is advisable to optimize and standardize these diagrams in the manuscript.

Some references lack standardized formats, urging further uniformity and standardization.

Reviewer #3

(Remarks to the Author)

The study conducted by Xiao et al. revealed that neural ensembles in the medial entorhinal cortex (MEC) responsible for encoding spatial experiences exhibit transient reactivation during NREM sleep, coinciding with isolated theta waves. Additionally, the authors observed that the nucleus reuniens (RE) in the midline thalamus demonstrates typical theta wave activity during NREM sleep, which is highly synchronized with the theta waves in the MEC. Through the application of a closed-loop optogenetic manipulation technique, the authors effectively inhibited the RE-MEC pathway, thereby suppressing isolated theta waves. This intervention led to impaired reactivation and compromised memory consolidation following a spatial memory task. These findings indicate that theta waves originating from the ventral midline thalamus play a crucial role in initiating memory reactivation. The manuscript is well-written, the figures are clearly presented, and the data support the conclusions. Knowledge gained from this study provides new information on the role of the midline thalamus in regulating memory consolidation. A few minor points listed below need to be further addressed.

1. For extended data fig2D, the data presented are the cell numbers in different brain regions. The authors should measure the size of each region and calculate the density of dsRed-labeled cells.
2. In line 214, what is the exact duration of "a few milliseconds"? Please include the latency of light-evoked EPSC in excitatory and inhibitory neurons.
3. What are the oEPSC responses of interneurons to blue light stimulation at different frequencies? Please also include the sample traces next to extended data fig4B.
4. What is the firing rate of excitatory neurons under basal conditions? Is 20 Hz stimulation considered too artificial, leading to a drop in the fidelity of light-evoked spikes after increasing the laser frequency?
5. Since fig2K shows the stimulation at 4 different frequencies, it would be appreciated to also include the sample traces of membrane voltage following 10Hz light stimulation under the i-c mode.
6. Please include the averaged bars of amplitude for each group in fig2G and 2I. Line 231: "These results suggest that MEC excitatory glutamatergic neurons, rather than inhibitory interneurons, mainly integrate monosynaptic and excitatory inputs from RE at theta frequency band in vitro." This statement requires clarification, as depicted in fig2F-2K, where it is evident that over half of the interneurons in the MEC receive excitatory inputs from RE (with the averaged amplitude of oEPSCs appearing comparable between Glu and IN groups, and two cells exhibiting oEPSCs larger than 40 pA). Moreover, light stimulation resulted in action potentials following 5Hz stimulation, albeit with a low probability, indicating the potential involvement of a small subset of interneurons in the circuit function, possibly exerting a feed-forward inhibition on the excitatory glutamatergic neurons. Please revise the sentence accordingly.
7. Line 239: Instead of "high resting potential," use "hyperpolarized" for greater clarity.
8. Line 1220: The phrase "response to light pulses" may be confusing since no light is applied in the figure. Please rephrase this sentence to avoid confusion.
9. Line 1231: "recooded" should be corrected to "recorded."
10. Line 283: The text mentions CNO at 5 μ M, but the label in fig4B is inconsistent. Please provide consistency between the

text and the figure.

11. Was the activity of cells in the MEC inhibited after bath application of CNO in the slice?

12. Extended Data Fig6D demonstrates that delta power was increased in the ArchT group compared to eYFP mice. Could delta power also be related to memory regulation?

13. It would be appreciated if the power density analysis of NREM and REM sleep during post-training were included in Extended Data Fig6.

14. In fig5B, what do the black and blue/purple traces represent? Please add details to the legends.

15. For closed-loop Optogenetic Intervention, how do the authors avoid applying light to REM sleep, considering it also consists of theta power? Could you please add more details to the methods?

Version 1:

Reviewer comments:

Reviewer #1

(Remarks to the Author)

The authors have fully addressed my concerns, therefore the manuscript is suitable for publication in its current form.

Reviewer #2

(Remarks to the Author)

I appreciate the significant enhancements made to the study by addressing my concerns and supplementing it with additional examinations and analysis. I have no further questions and congratulate the authors on an exciting article.

Reviewer #3

(Remarks to the Author)

In the revised manuscript, the authors have addressed my concerns, and the manuscript is ready to proceed for publication.

Open Access This Peer Review File is licensed under a Creative Commons Attribution 4.0 International License, which permits use, sharing, adaptation, distribution and reproduction in any medium or format, as long as you give appropriate credit to the original author(s) and the source, provide a link to the Creative Commons license, and indicate if changes were made.

In cases where reviewers are anonymous, credit should be given to 'Anonymous Referee' and the source.

The images or other third party material in this Peer Review File are included in the article's Creative Commons license, unless indicated otherwise in a credit line to the material. If material is not included in the article's Creative Commons license and your intended use is not permitted by statutory regulation or exceeds the permitted use, you will need to obtain permission directly from the copyright holder.

To view a copy of this license, visit <https://creativecommons.org/licenses/by/4.0/>

Reviewer #1 (Remarks to the Author): The neural mechanisms driving reactivation of neural ensembles during NREM sleep remain poorly understood. In introduction the author emphasized that the midline thalamic neurons display distinct characteristics compared to these wakefulness-promoting neurons. These midline thalamic neurons exhibit burst firing during NREM sleep and thus may play a crucial role in driving reactivation of neural ensembles associated with memory consolidation during NREM sleep. Combining multi-channel single-unit recording, closed-loop optogenetic intervention, chemogenetic intervention, fiber photometry recording, whole-cell patch clamp recording and other methods, this study demonstrated that the neural ensembles in the medial entorhinal cortex (MEC) that encode spatial experiences exhibit transient high frequency firing pattern during NREM sleep. These results suggest that isolated theta waves of the nucleus reuniens (RE) in the midline thalamus serve as a reliable sign of reactivation. Closed-loop optogenetic inhibition of RE-MEC pathway specifically suppressed these isolated theta waves, resulting in impaired reactivation and compromised memory consolidation following a spatial memory task. Taken together, these results reveal that the midline thalamus has a unique role in memory consolidation during NREM. Although the study offers novel perspectives on the mechanisms by which sleep enhances memory consolidation, the functional role of RE-MEC pathway is not sufficiently demonstrated with the current data and thus need further supporting evidence. Moreover, more detailed method descriptions are required as pointed below.

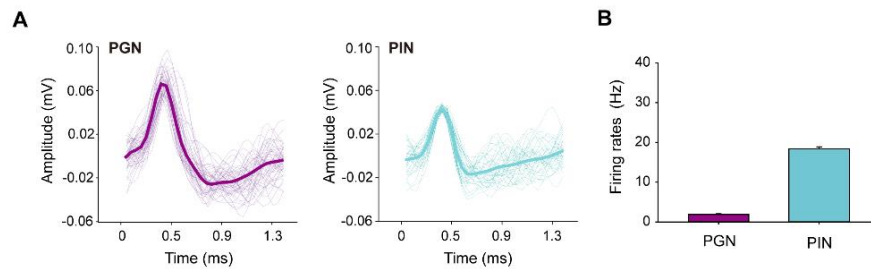
R: We really appreciate your appreciation of our work, as well as the precious comments and advice. Those comments are all valuable for revising and improving our manuscript.

Major comments:

1. According to the firing pattern detected by principal component during training phase (left) and post-training phase in Fig 1E, MEC cell ensembles with highest principal component (PC) intensity and corresponding reactivation strength fired at high frequency, which were more likely to be interneurons. However, subsequent results indicated that MEC excitatory glutamatergic neurons, but not inhibitory interneurons, efficiently integrate excitatory inputs of RE at theta frequency band in vitro (Fig 3). Please explain the contradictory results. For this purpose, I suggest to distinguish inhibitory neurons and excitatory neurons of MEC in Fig 1. It will help to determine the main neural types involved in this reactivation.

R: We deeply appreciate the reviewer's valuable comment and suggestion. According to the previous studies (Peyrache et al., Nature Neuroscience, 2009; Kim et al., Cell, 2019), we used principal component analysis to identify the firing patterns, followed by the computation of reactivation strength. In fact, this method captures firing patterns encompassing all neurons without specifically distinguishing excitatory and inhibitory neurons. According to the reviewer's suggestion, we have further performed additional analyses, and distinguished putative interneurons (PIN) and putative glutamatergic neurons (PGN) (Lin et al., eLife, 2021;

Chen et al., *Cerebral Cortex*, 2018). The PIN had high firing frequency and narrow width of spike waveforms with the half-spike width < 0.4 ms, while the PGN had broad waves and low firing frequency (Refer to Rfig. 1).



Rfig. 1. Classification of putative glutamatergic neurons (PGN) and putative interneurons (PIN) in the MEC.

A Characteristic of the spike waveforms of PGNs (left) and PINs (right).

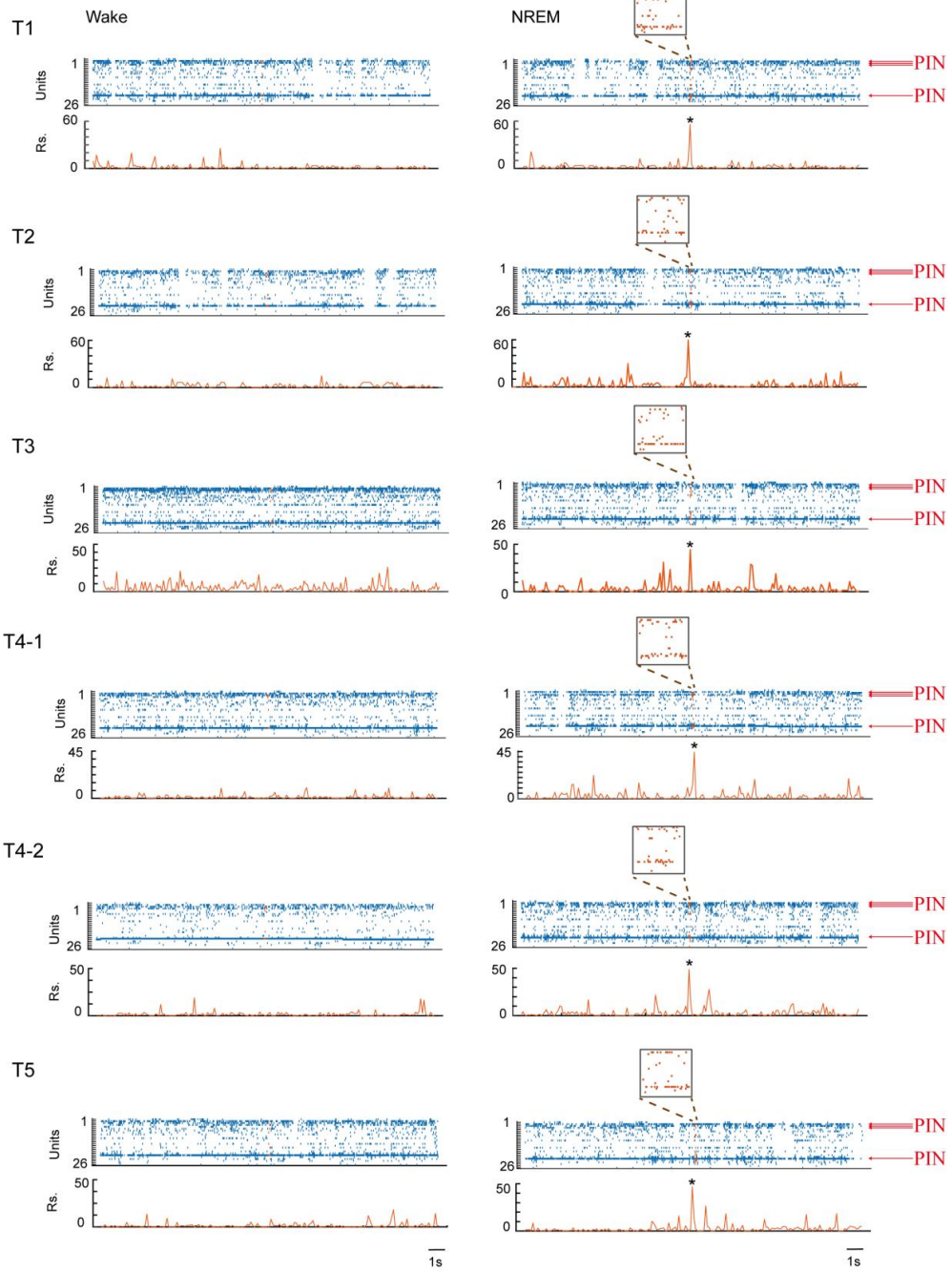
B Firing rates of PGNs and PINs, noting that PINs fire at a high frequency than PGNs.

In our study, a total of 117 and 129 neurons were recorded on day 1 and day 2 from six mice. Among them, the number of PIN was 8 and 10 and, on average, PIN only accounted for 18% and 13% on day 1 and day 2, respectively. The majority of the remaining neurons consisted of PGN (Refer to the Table 1). Specifically, each firing pattern and its cell type compositions are shown in the Rfig. 2. These results suggest that the detected firing patterns of cells undergoing reactivation is still dominated by glutamatergic neurons, with only a minority of inhibitory interneurons.

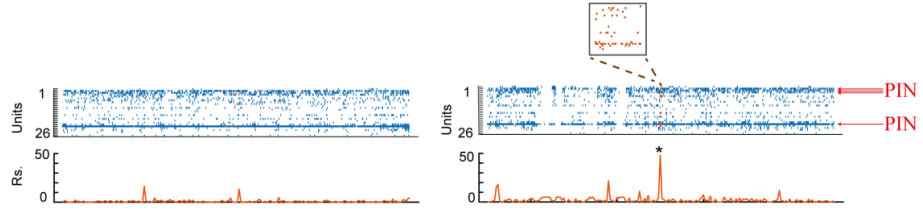
In Figure 1E of the original manuscript, we presented a firing pattern consisting of a subset of cells with high firing frequencies only, which led the reviewer to mistakenly assume that the reactivated neurons were predominantly interneurons. We sincerely apologize for this inappropriate presentation. In fact, the detected firing pattern should include a record of all neurons. We have corrected this issue by showing that firing patterns and the corresponding all recorded neurons (See the Fig. 1E in the revised manuscript). Furthermore, we clearly describe the number and proportion of excitatory neurons and interneurons that contribute to the firing patterns in the revised manuscript (See lines 110-111 on page 6).

Table 1. A summary for the number and type of the recorded neurons in the MEC

	Day1			Day2		
	Total num.	Num. of PIN	Per. of PIN	Total num.	Num. of PIN	Per. of PIN
<i>NO.281</i>	26	4	15.38%	25	2	8.00%
<i>NO.2108</i>	14	2	14.29%	20	3	15.00%
<i>NO.290</i>	9	1	11.11%	22	1	4.55%
<i>NO.291</i>	17	0	0.00%	25	0	0.00%
<i>NO.53</i>	31	1	3.23%	18	0	0.00%
<i>NO.A40</i>	20	2	10.00%	19	2	10.53%
In total	117	10	17.55%	129	8	12.55%

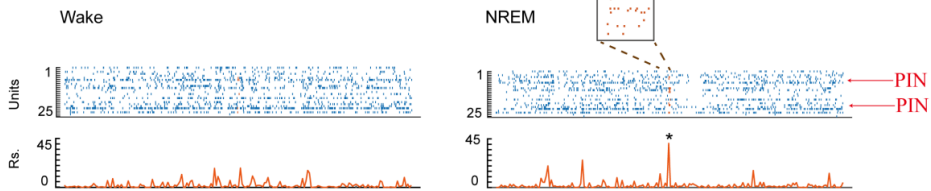


T6

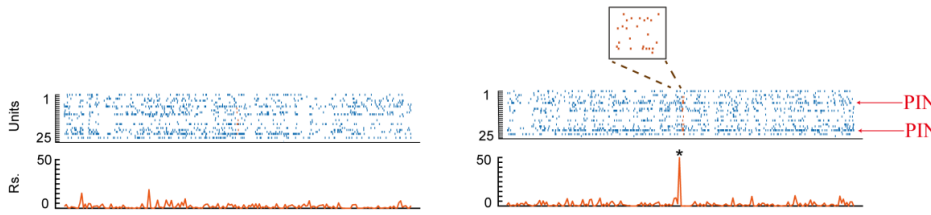


No.281.day2

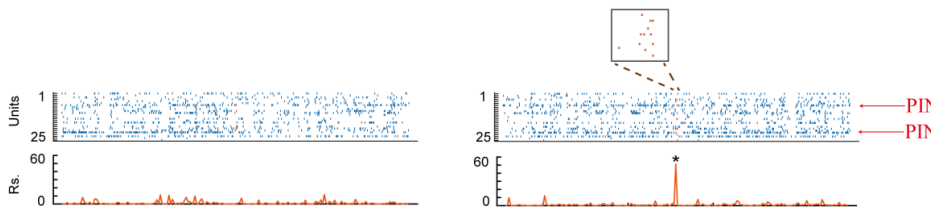
T2



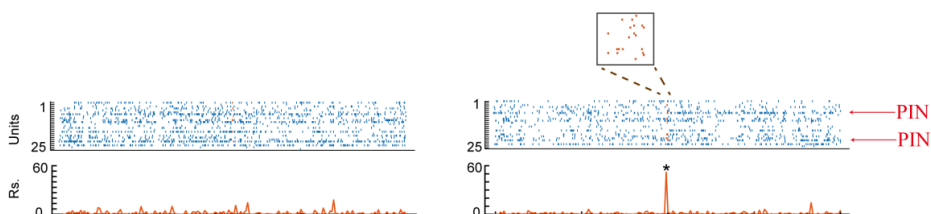
T3



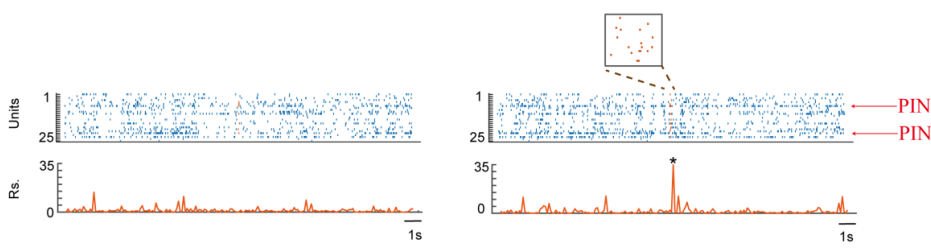
T4

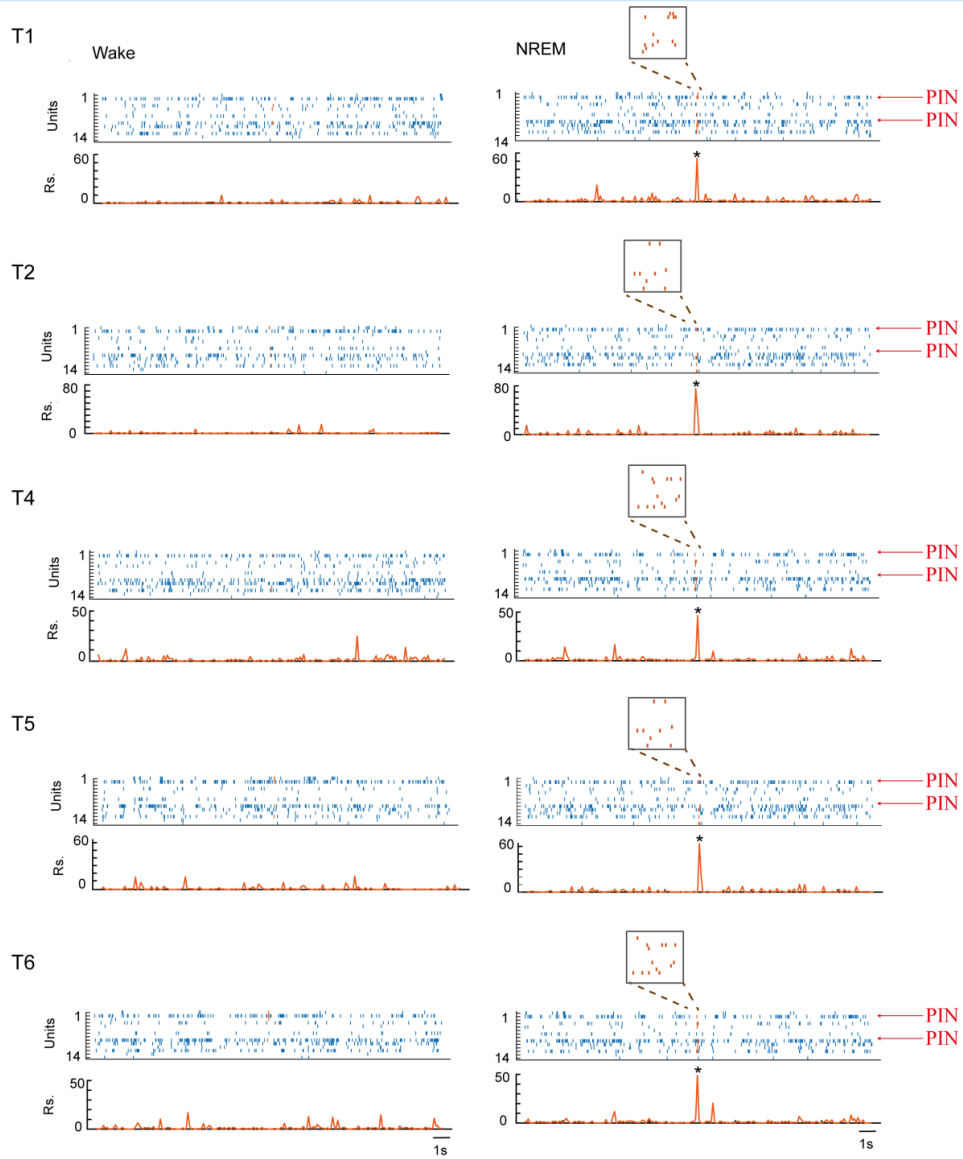


T5

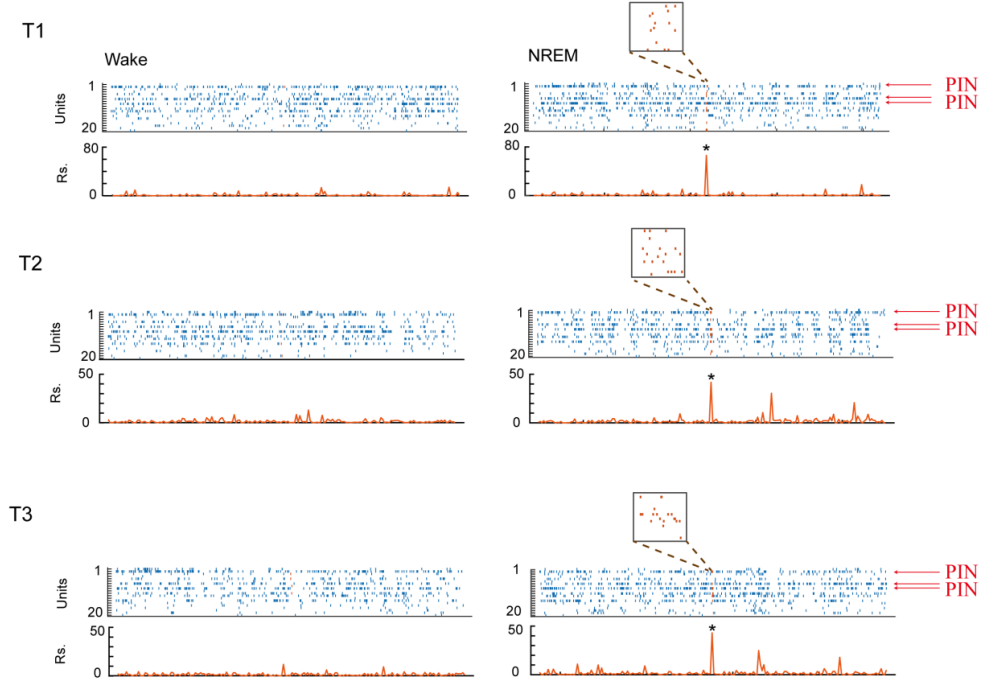


T6

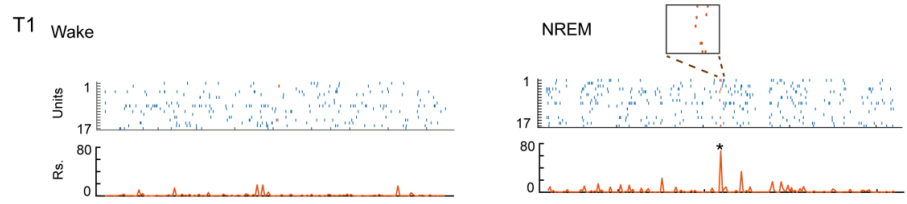




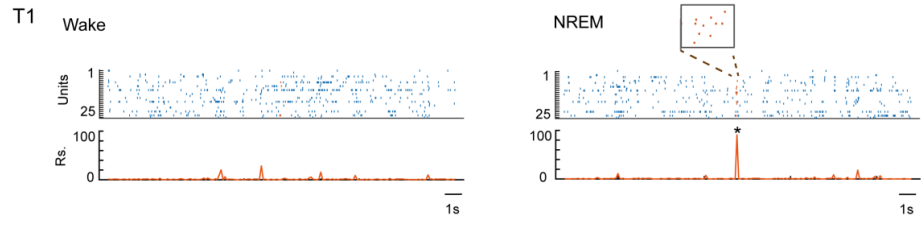
No.2108.day2



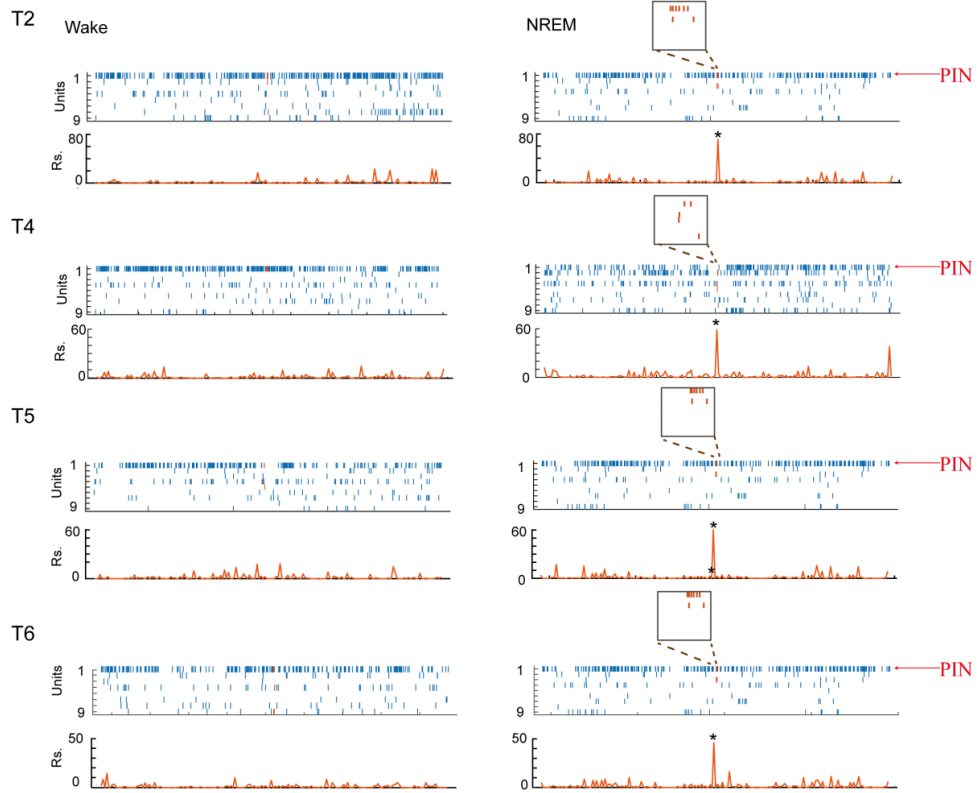
No.291.day1



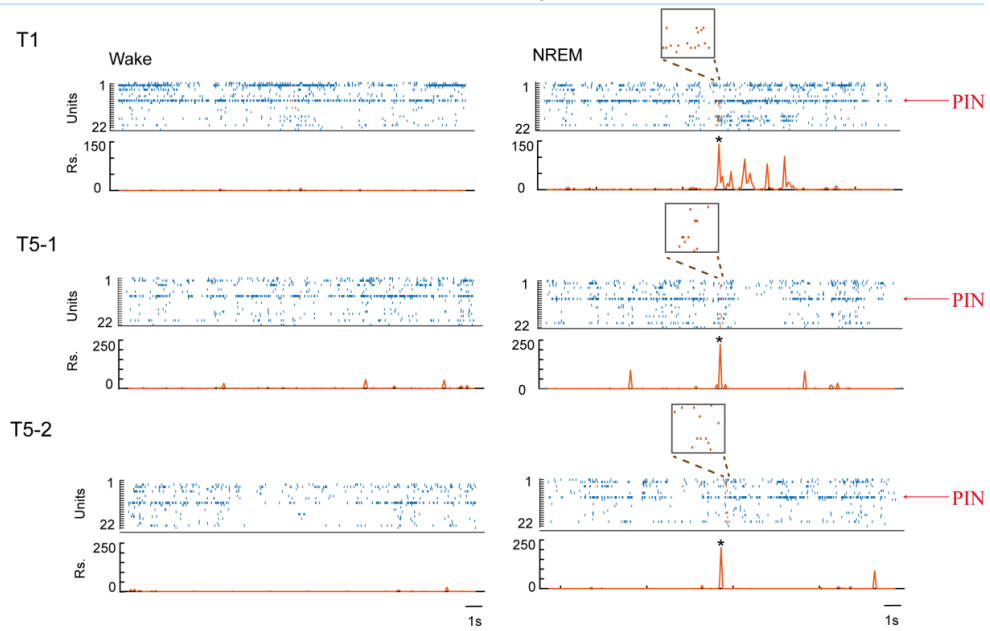
No.291.day2



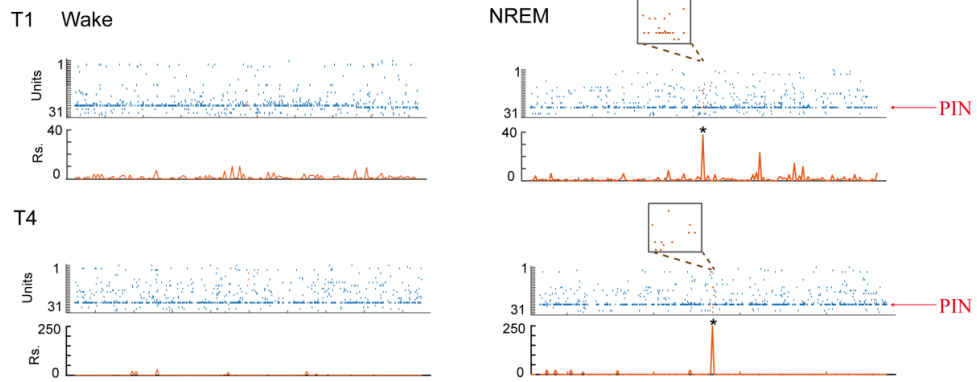
No.290.day1



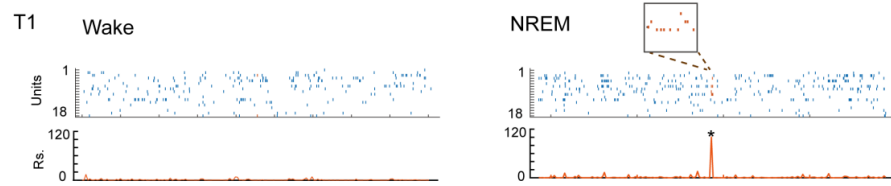
No.290.day2



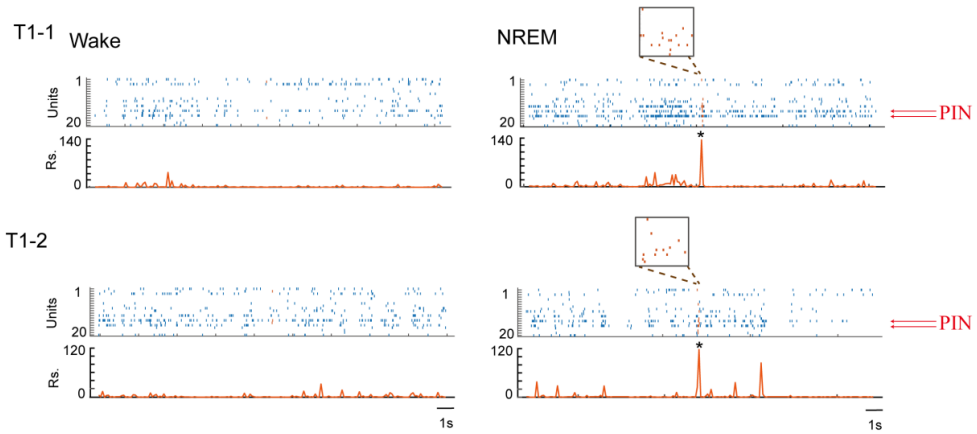
No.A53.day1

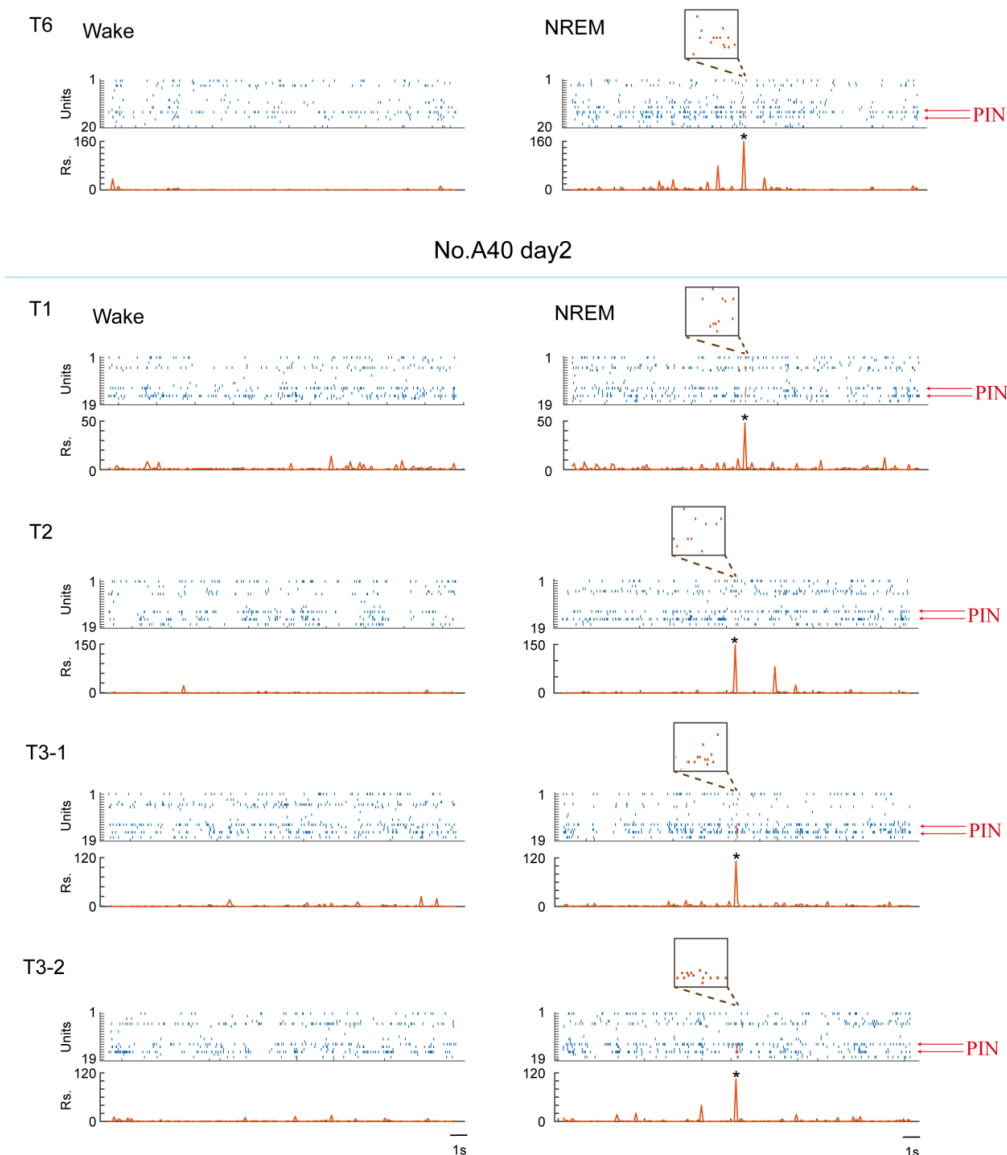


No.A53.day2



No.A40.day1





Rfig. 2. The firing patterns detected, along with the corresponding neurons and reactivation strength during post-learning awake and NREM sleep are presented.

An enlarged view of the detected firing patterns is shown in the inset box, where putative interneurons (PIN) are indicated by red arrows. The firing patterns detected in which trials are represented by T1-6.

On the other hand, although fewer interneurons formed the firing patterns, their reactivation also occurred during NREM sleep. Because our patch-clamp recordings demonstrated that stimulation of RE inputs more effectively excite excitatory glutamatergic neurons, hence, reactivation of PIN appears to contradict these patch-clamp findings. In fact, the interneurons receive a large amount of input from local excitatory neurons within the superficial layers of the MEC (*Fuchs et al., Neuron, 2016*). Therefore, one explanation for this discrepancy is that the reactivation of glutamatergic neurons triggered by RE input during

NREM sleep may subsequently drive the reactivation of interneurons through this local circuit in the MEC *in vivo*. We have added the discussion on this issue as follows (See lines 416-422 on pages 20 and 21).

*"Although the *in vitro* patch clamp experiment revealed that RE strongly excites MEC excitatory neurons, it is important to consider that interneurons receive a substantial amount of input from local excitatory glutamatergic neurons within the MEC region. Therefore, the reactivation of excitatory neurons triggered by RE input during NREM sleep may subsequently drive the reactivation of interneurons through this local circuit in the MEC *in vivo*."*

2. Simultaneous analysis of EEG and EMG of this study showed that animals spent most time in NREM sleep and very little time in rapid eye movement (REM) sleep (Extended Data Fig. 1A-B, line of 108-110), therefore, the study focused only on NREM sleep in the subsequent analyses. However, numerous researches before had proved that theta waves were mostly present during REM sleep (Buzsáki, 2002; Jouvet, 1969, see references below for detail) and during various types of locomotor activities (Vanderwolf, 1969). Moreover, previous studies had even shown that theta waves were absent in the immobile animal (Bland, 1986). Considering so many opposite conclusions, the author need to explain these contradictory results anyway.

References:

Bland, B. H. (1986). The physiology and pharmacology of hippocampal formation theta rhythms. *Prog Neurobiol*, 26(1), 1-54. doi: 10.1016/0301-0082(86)90019-5

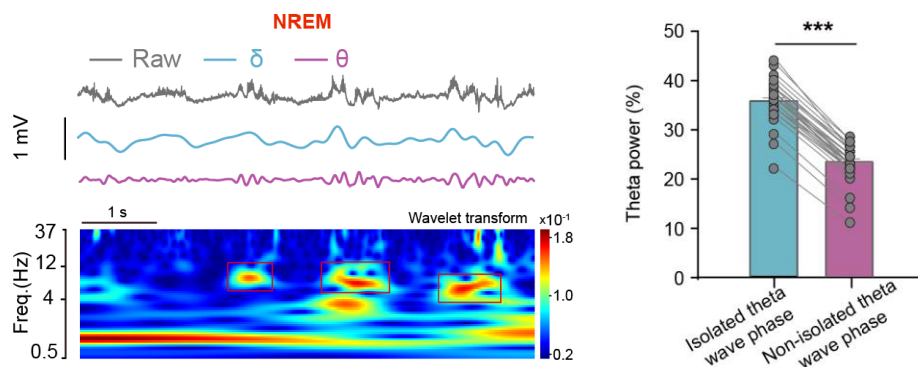
Buzsáki, G. (2002). Theta Oscillations in the Hippocampus. *Neuron*, 33(3), 325-340. doi: [https://doi.org/10.1016/S0896-6273\(02\)00586-X](https://doi.org/10.1016/S0896-6273(02)00586-X)

Jouvet, M. (1969). Biogenic amines and the states of sleep. *Science*, 163(3862), 32-41. doi: 10.1126/science.163.3862.32

Vanderwolf, C. H. (1969). Hippocampal electrical activity and voluntary movement in the rat. *Electroencephalography and Clinical Neurophysiology*, 26(4), 407-418. doi: 10.1016/0013-4694(69)90092-3

R: We thank the reviewer to point out this issue. Although theta oscillations in the MEC have been observed when animal displayed exploratory activity during awake state (Lepperod *et al.*, *Sci Adv.* 2021; Carpenter *et al.*, 2017, *Sci Rep.* 2017), the previous reports on the oscillatory activity patterns during NREM sleep in the MEC have not yet been provided. In this study, we simultaneously recorded EEG/EMG and local field potentials (LFP) of the MEC, strictly staging NREM sleep following the previous study protocol (Li *et al.*, *Nature communications*, 2018; Zhang *et al.*, *Current Biology*, 2024). Utilizing the conventional energy spectrum analysis method for LFP (Chen *et al.*, *Cerebral Cortex*, 2018), indeed, we found that delta waves were prominent in the MEC during NREM sleep. Further analysis showed that there was also strong oscillatory activity in the theta frequency band of 4-12 Hz. These theta events occurred intermittently with short-term duration lasting about 300 ms, and were coupled with upstates

of delta waves (Because the short duration of these theta events, they are called isolated theta waves). During phase of isolated theta waves, the proportion of theta band power reaches 35%, which is significantly higher than that of non-isolated theta wave phase (Refer to Rfig. 3).



Rfig. 3. Representative trace of LFP recorded in the MEC and corresponding power spectrum during NREM sleep. Left, Gray: raw trace; Red: filtered delta; Purple: filtered theta. Theta events detected is framed in the red rectangle box. Right, Distributions of MEC LFP power in the theta band during isolated theta event and non-isolated theta wave phases (Mann-Whitney Rank Sum Test, $n = 18$ for each group, $U = 129$, $P = 0.3017$). $***P < 0.001$.

The previous studies mentioned by the reviewer have exclusively focused on the hippocampus. Notably, these studies consistently demonstrate that theta waves are predominantly present during REM sleep and locomotor activities in the hippocampus, while sharp wave ripples prevail during NREM sleep instead of theta oscillations. Additionally, a review of the literature reveals that the prefrontal cortex exhibits theta oscillations during wakefulness, but displays delta-nested spindle activity rather than sharp wave ripples during NREM sleep (Staresina et al., *Nature Neuroscience*, 2023). These findings suggest that different brain regions may exhibit distinct oscillatory activities during NREM sleep.

Nevertheless, we did not describe in detail the differences between MEC theta activity during NREM sleep, and the theta activity in the hippocampus, thus raising questions from the reviewer. To address this issue, we further elaborate on the observed theta characteristics and add the relevant discussion as follows (See lines 207-214 on pages 10 and 11).

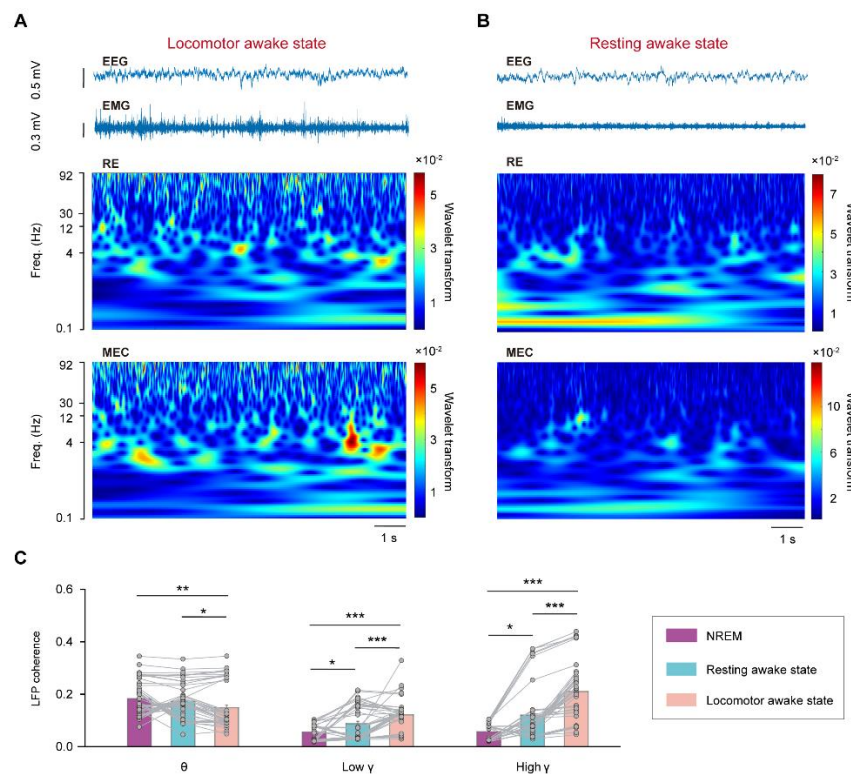
“Of note, the occurrence of theta oscillations in the hippocampal formation is primarily observed during movement and REM sleep. During movement, the frequency of theta oscillations in the hippocampus was notably high, surpassing 8 Hz. Conversely, synchronized theta activity between RE and MEC exhibited a lower frequency of less than 7 Hz, with these isolated theta oscillations being brief in duration lasting only a few hundred milliseconds. These findings indicate that isolated theta oscillations in MEC during NREM sleep possess distinct characteristics compared to those recorded during wakefulness.”

3. It's an interesting observation that the synchronized activity shifted from theta frequency band to gamma frequency band when entering the wakening state (Extended

Data Fig. 3A-C). Then, will this dynamic change in oscillatory still occurred if the waking state is further subdivided into locomotor state or resting state? For example, this change occurred in both locomotor and resting state or only occurred in one of the two states?

R: In the original manuscript, we found that the synchronized activity in theta frequency band decreased, while the synchronized activity in gamma frequency band enhanced when entering the waking state, indicating a change in the synchronized activity between RE and MEC across NREM sleep and wakefulness. Based on reviewer's comment, we have carried out new analyses, and the waking state is further subdivided into locomotor state and resting awake state. The synchronized activity in the low gamma and high gamma oscillations between the RE and MEC was enhanced both during the locomotor state and resting awake state, compared to NREM sleep. Whereas this synchronization activity in these gamma frequency bands was highest during locomotor state. In contrast, for theta oscillations, the synchronized activity decreased during the locomotor state; however, no significant difference was found between resting awake state and NREM sleep (*Refer to Rfig. 4*).

The new analysis findings indicate that this change occurs in both states. The results of these new analyses have been added to the revised manuscript (*See Extended Data Fig. 5 in the revised manuscript*).



Rfig. 4. LFP coherence in different bands between RE and MEC during locomotor, resting awake state and NREM sleep.

A, B Representative raw EEG-EMG traces, LFPs in the RE and MEC during locomotor awake state (**A**) and resting awake state (**B**).

C LFP coherence in the RE and MEC during NREM sleep, locomotor awake state and resting

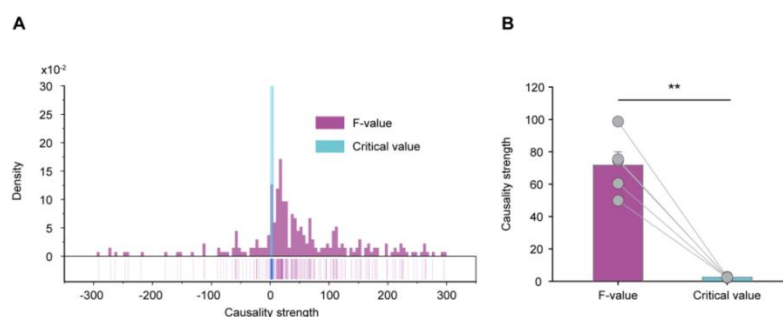
awake state. Data are presented as mean \pm s.e.m. (Friedman Repeated Measures Analysis of Variance on Ranks, $n = 51$ channels. Theta: $q = 7.569$, $P = 0.023$; low gamma: $q = 20.118$, $P < 0.001$; high gamma: $q = 60.118$, $P < 0.001$).

4. In the line of 203-205 evidences were insufficient to support the results stated. More experiments and analyses were needed to prove the temporal directionality between RE and MEC in memory information transfer, such as Granger causality analysis, etc.

R: Many thanks for your constructive suggestion. Of note, in the original version of our manuscript, we have performed closed-loop optogenetic experiments to prove the temporal directionality. We found that closed-loop optogenetic inhibition of the RE-MEC pathway effectively reduced theta wave power, decreased the coupling strength of the delta wave and isolated theta waves during NREM sleep, and altered the preferred phase in which isolated theta waves are coupled to delta waves (See Fig. 6 C, D and Extended Data Fig. 12 C, D in the revised manuscript). These results suggest that RE plays a causal role in driving the isolated theta waves of the MEC during NREM sleep.

To further prove the temporal directionality, we conducted new Granger causality analysis in line with the reviewer's suggestion. We calculated F-value, reflecting the strength of the temporal directionality from the RE to MEC, and critical value of the F-value distribution at $P = 0.05$ based on the previous study (Granger et al., *Econometrica*, 1969). The distribution plot of the F-values and corresponding critical values reveals that a majority of the F-values exceed the critical values (See Rfig. 5A). On average, the calculated F-value is approximately 71.8 ± 8.2 ($n = 5$ mice), which is significantly larger than the critical value of 2.4 ± 0.1 (See Rfig. 5B). These analysis results further indicate that most theta events occur initially in RE and may subsequently be transmitted to MEC, which proves the temporal directionality from RE to MEC.

We have included the results of these new analyses in the revised manuscript (See Extended Data Fig. 6 in the revised manuscript).



RFig. 5. Theta waves propagate from RE to MEC proved by Granger analysis.

A Distribution of the F-value and the critical value calculated by the Granger analysis for the detected theta events.

B Statistical analysis of the calculated F-value and the critical value. Data are presented as mean \pm s.e.m. (Paired t test, n = 5 mice, $t_4 = 8.488$, $P = 0.001$).

5. Did the MEC reactivated cell ensembles include grid cells? If yes, did the reactivation only occurred in grid cells?

R: We thank the reviewer for pointing out a very interesting issue. Our study mainly focuses on mechanisms underlying the MEC-related spatial memory consolidation during NREM sleep. In the present research system, it does not involve the concept of the grid cells. To involve the topic of grid cells, specialized behavioral paradigm of the open field (1 m \times 1 m) behavioral test is required (Gardner et al., *Nature Neuroscience*, 2019; Trettel et al., *Nature Neuroscience*, 2019). However, in our study, a six-arm maze behavioral paradigm was mainly used to examine MEC-related spatial memory. Because of the different behavioral paradigms, we are very sorry about that we couldn't further isolate grid cells in our behavioral paradigm.

After reviewing the literatures, in fact, we found that previous studies have recorded ensembles of grid cells in superficial layers of MEC during actively exploratory behaviors and subsequently detected their activity during NREM sleep. The patterns of spike-time correlations that reflected the spatial tuning offsets between these grid cells during active exploration were reactivated during the subsequent NREM sleep (Trettel et al., *Nature Neuroscience*, 2019). Considering that, in our spatial memory task, it also includes the process of spatial exploration, therefore it is reasonable to speculate that MEC reactivated cell ensembles may also include grid cells in our study.

Anyhow, the question you have posed is indeed intriguing, and we would like to express our sincere gratitude for your contribution. In future endeavors, we will design more specific experiments to address this problem. In response to this concern, we have incorporated additional discussions in the revised manuscript as follows (*Refer to lines 423-430 on page 21*).

“Previous studies have recorded ensembles of grid cells in superficial layers of MEC during active exploratory behaviors and NREM sleep. The patterns of spike-time correlations that reflected the spatial tuning offsets between these grid cells during active exploration was also observed during the NREM sleep. The current study primarily employed a six-arm maze behavioral paradigm to investigate MEC-related spatial memory, which may not be optimal for detecting grid cells. Further investigation is required to determine whether the identified isolated theta oscillations drive the reactivation of grid cells during NREM sleep.”

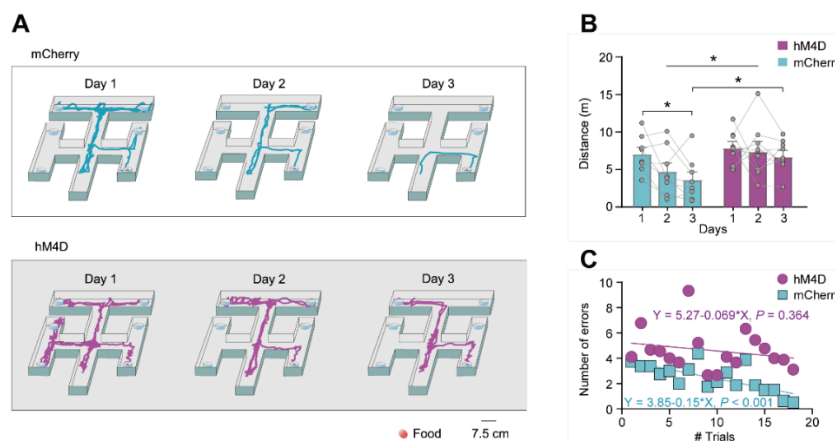
6. Fig 4H: please explain the obvious difference in the baseline behavior performance of the mCherry-expression mice and hM4Di-expression mice on the first day. Will this difference affect your present findings and conclusions? Or the findings could be related to this baseline difference?

R: We appreciate you for this valuable comments. Indeed, running distance seem to be longer on the first day in hM4D group than the control group. After checking the raw data,

we found that there are two of the mice in the hM4D group moving a very long distance (14.0 m of NO.510, 18.3 m of NO.488), much higher than the overall average, while the other 5 mice in the hM4D group all moved between 5-7 m. It can be seen that this obvious difference in the baseline was mainly caused by these two animals. Further examination of the recorded behavioral videos, these two animals exhibited remarkably intense stereotypic behavior, repeatedly exploring only one arm of the maze, indicating a significant impairment in their motivation for exploration (See the movies in the supplemental files). Consequently, they were deemed unsuitable for further examination of their spatial memory. We are sorry about that we are not detect this problem in the initial version of our manuscript.

In view of this, we conducted new experiments by increasing the sample size in the hM4Di group. We added four new mice to the hM4D group and excluded the two animals with large variation. The movement distance of the four newly added animals was 5-7 m, which was at a normal level. In the end, 8 control mice and 9 mice in the hM4D group were included for analyses. We found that no discrepancies in the running distance were observed in baseline differences on the first day following animal addition. Under this condition, our findings still demonstrated that chemogenetic inhibition of the RE-MEC pathway impairs memory consolidation as evidenced by longer running distances to locate the target on both second and third days after intervention (Refer to Rfig. 6).

In the revised version of the manuscript, these new results regarding the chemogenetic inhibition of the RE-MEC pathway have been included in the revised manuscript (See Fig. 5 in the revised manuscript).



Rfig. 6. Chemogenetic inhibition of RE-MEC pathway after training impaired spatial memory.

A Representative trajectories of the mouse in the mCherry (top) or hM4D (bottom) group searching for food in the six-arm maze. Training for 3 days, 6 trials per day.

B The distance that animals of the mCherry and hM4D groups traveled in the maze to acquire food each day. Gray line represents individual mouse. Data are presented as mean \pm s.e.m. (Two-

way RM ANOVA, $n = 8$ mice for mCherry group, $n = 9$ mice for hM4D group; mCherry vs hM4D, $F_{1,15} = 4.702$, $P = 0.0466$; days factor: $F_{2,30} = 4.515$, $P = 0.0193$; interaction, $F_{2,30} = 1.192$, $P = 0.3175$). $*P < 0.05$.

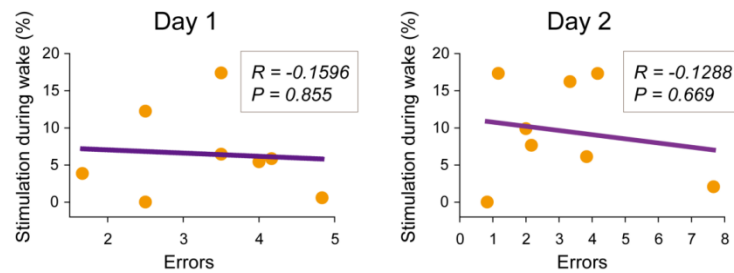
C Average number of errors that animals in the mCherry and hM4D groups made when searching for food during 6 trials each day. Blue circles or purple blocks represent mean value for each trial of mCherry ($n = 8$ mice) or hM4D group ($n = 9$ mice). Trend lines are the least-square fits to the data.

7. How long did the closed-loop optogenetic intervention totally last? How did a closed-loop optogenetic program stop when the animal was not under the NREM state? Did the author applied the closed-loop optogenetic intervention selectively under the NREM state. If not, how to rule out that the theta wave was also interfered when the animal's state changed from NREM to wakefulness? Please answer these questions in detail in both the Results and Method section.

R: We are sorry about the lack of comprehensive information. The closed-loop optogenetic intervention was performed based on the previous study (Qin et al., *Neuron*, 2022). The subject mouse was returned to the home cage immediately and the EEG-EMG recording was monitored to manually identify NREM episodes across the following 1 h. NREM sleep was defined by high amplitude and low frequency EEG activity, as well as low amplitude EMG activity. Once the mice entered NREM sleep, the laser generator was turned on, and the closed-loop system would specifically detect theta oscillations during NREM sleep to trigger the optogenetic stimulation. After quantification, closed-loop optogenetic intervention totally last 263 ± 29 s and 266 ± 78 s for control group ($n = 9$ mice), and 241 ± 36 s and 244 ± 36 s for ArchT group ($n = 8$ mice) on day 1 and 2, respectively. 93.8% and 90.5% of optogenetic stimulation were applied during NREM sleep for ArchT group on day 1 and day 2, respectively. These results suggest that intervention was applied mainly during NREM sleep.

Although closed-loop optogenetic approach is widely used, nonetheless, it is still not absolutely perfect, that is, the 6.2% and 9.5% of the optogenetic interventions were applied outside the NREM sleep in day1 and day 2. In fact, with regard to the electrophysiological data, our analysis specifically focuses on the effects of optogenetic inhibition of RE-MEC during NREM sleep only. Moreover, we also investigated the association between wakefulness stimuli and memory performance, but no significant correlation was found between the duration of stimuli during wakefulness and the number of errors (Refer to Rfig. 7). These results imply that reactivation of spatial memory is primarily driven by RE inputs during NREM sleep rather than wakefulness.

In the revised manuscript, we have added this information in detail in the revised manuscript (See lines 767-775 on page 42).



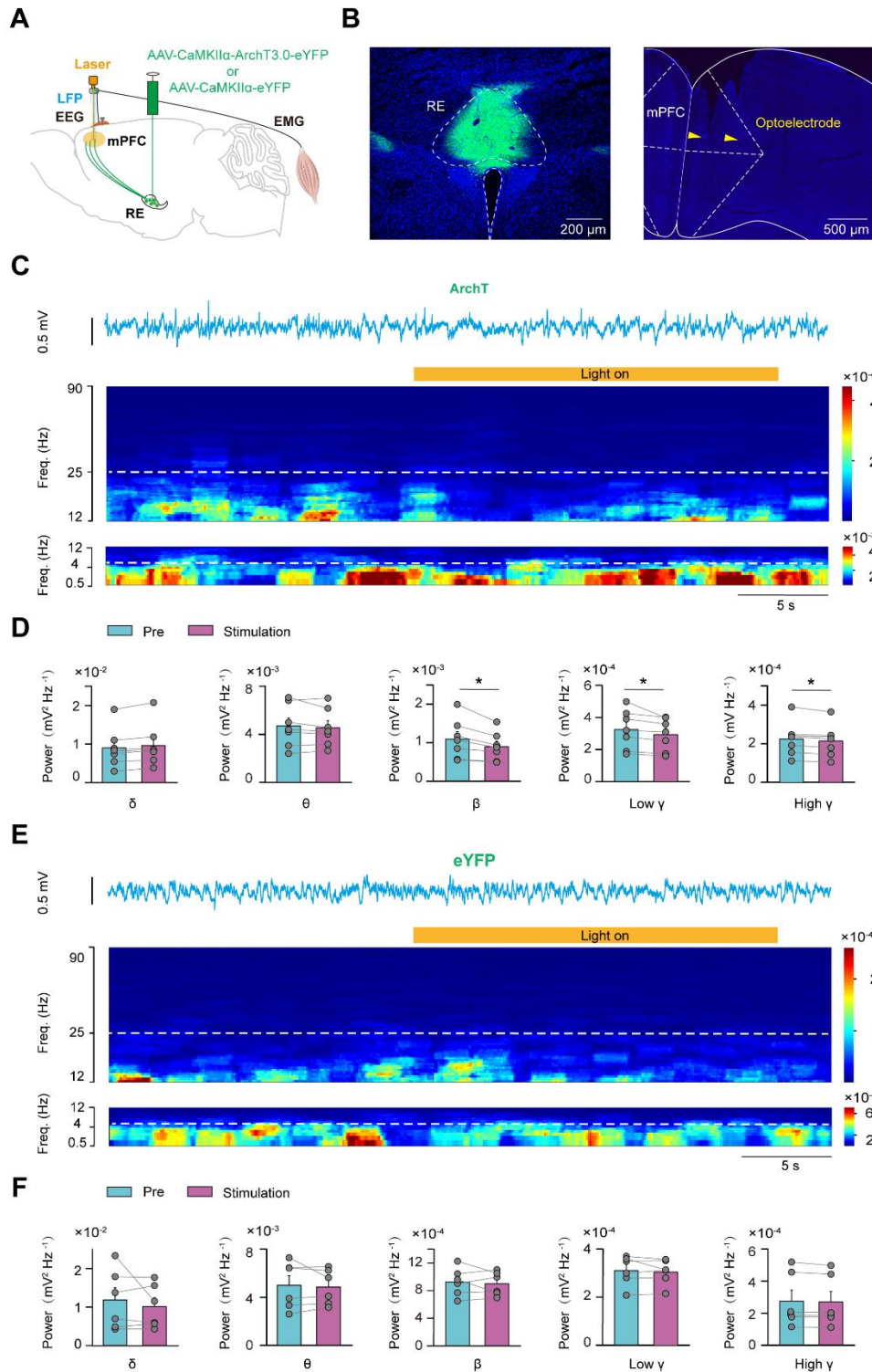
Rfig. 7. Linear analysis of the proportion of light stimulation delivered during awakening period and the spatial memory performance.

Note that number of errors was not positively correlated with the proportion of light stimulus that fell during wake, indicating the low proportion of light stimulation during arousal is not sufficient to influence animals' spatial learning (n = 8 mice for ArchT group were included).

8. Cited studies indicate that cells in the midline thalamic nuclei can generate burst-mode discharges lasting about hundreds of milliseconds during NREM sleep (in the line of 181 - 183). Did the author obtained any experimental evidence supporting that RE burst discharge can drive neocortical high-frequency oscillations, both in MEC and PFC?

R: We are grateful to the reviewer's suggestion. In addition to the finding that RE can drive high-frequency isolated theta oscillations in the MEC, we conducted new experiments to investigate whether RE affects high-frequency oscillatory activities in the mPFC during NREM sleep. We found that mPFC is different from MEC in that it mainly shows beta (12-25 Hz) high-frequency oscillatory activity during NREM sleep. After inhibition of this pathway, the high-frequency oscillations decreased significantly, especially the beta oscillation activity, which decreased by 18%. However, we found that inhibition of the RE-mPFC pathway did not affect the delta and theta oscillations. In the eYFP control animals, light stimulation did not affect the neuronal network oscillatory activity in the mPFC (*Refer to Rfig. 8*).

These results suggest that in addition to affecting the theta oscillations of MEC, RE can regulate high-frequency beta oscillations of the mPFC during NREM sleep. Moreover, in different brain regions, RE may participate in memory consolidation through different network oscillation mechanisms. We have added these new results in the revised manuscript (*See Extended Data Fig.13 in the revised manuscript*), and a new discussion was added for this issue (*See lines 342-349 on page 17*).



Rfig. 8. Effects of optogenetic inhibition of RE-mPFC pathway on the network oscillations during NREM sleep.

A Schematic of optogenetic inhibition of the RE-mPFC pathway during NREM sleep.

B Representative image showing the expression of ArchT-eYFP in the RE (green, left) and the optoelectrode implanted in the mPFC (dotted yellow pane, right).

C, E Raw trace of LFP (top) recorded in the mPFC and corresponding power spectrum (bottom)

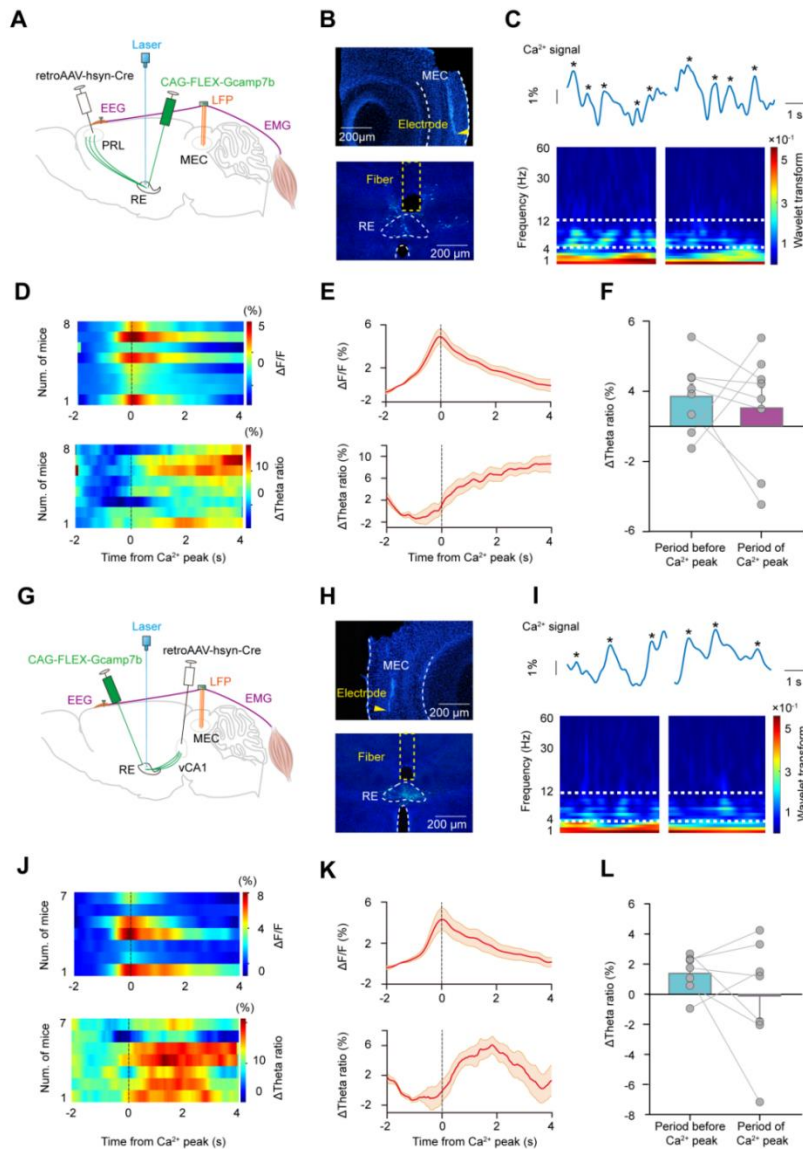
before and when yellow light was delivered to inhibit RE-mPFC pathway during NREM sleep of the ArchT (C) or eYFP (E) group.

D, F Statistic analysis of mPFC LFP in different bands before and when yellow light was delivered to inhibit RE-mPFC pathway during NREM sleep of the ArchT (D) or eYFP (F) group. (ArchT: n = 7 mice, paired t test or Wilcoxon Signed Rank Test. Delta: $t_6 = -2.026$, $P = 0.089$; theta: $t_6 = 1.026$, $P = 0.345$; beta: $t_6 = 3.496$, $P = 0.013$; low gamma: $Z = -2.366$, $P = 0.016$; high gamma: $t_6 = 3.475$, $P = 0.013$. eYFP: n = 6 mice, paired t test or Wilcoxon Signed Rank Test. Delta: $Z = -0.314$, $P = 0.844$; theta: $Z = 0.105$, $P = 1.00$; beta: $t_5 = 0.485$, $P = 0.648$; low gamma: $t_5 = 0.731$, $P = 0.498$; high gamma: $t_5 = 0.954$, $P = 0.384$). Data are presented as mean \pm s.e.m.

9. Fig 3: RE neuron projecting to the MEC labeled by calcium indicator GCamp7b are not selective for excitatory or inhibitory neurons. Then, it is necessary to conduct control experiments (brain region control) to better explain the strong correlation between calcium activities of projection neurons in RE and theta events power in MEC.

R: As one of the nuclei of midline thalamus, the main neuron type of RE is excitatory glutamatergic neurons, and it is generally believed that it does not contain inhibitory neurons (Vertes et al., *Neurosci. Biobehav. R.*, 2015). We are very sorry about that this information was not provided in our manuscript. We have revised this issue by adding this information in the revised manuscript (See line 179 on page 9).

In addition, we also carried out control experiments. According to the previous study (Ferraris et al., *Neurosci. Biobehav. R.*, 2021), RE mainly projects to three downstream target areas, including the MEC, hippocampal CA1 and mPFC. We further specifically recorded activities of the RE neurons projecting to the hippocampal CA1 and mPFC, and simultaneously collected LFP in the MEC. When the RE neurons projecting to either CA1 or PFC exhibited elevated calcium activity during NREM sleep, however, there was no concurrent increase in theta oscillations observed in the MEC, indicating a lack of correlation between the activity of RE neurons projecting to CA1 or PFC and theta oscillations in MEC (Refer to Rfig. 9). These control experiments further substantiate that only RE neurons projecting to MEC display a strongly positive correlation with MEC's isolated theta oscillations. These new results have been included in the revised manuscript (See Extended Data Fig. 9 in the revised manuscript).



Rfig. 9. MEC theta waves is not positively correlated with the activities of RE neurons projecting to mPFC or ventral CA1.

A, G Diagram for simultaneously fiber photometry recording of RE neurons projecting to mPFC (**A**) or vCA1 (**G**) as well as LFPs recordings in the MEC.

B, H Representative image showing RE neurons projecting to mPFC (**B**) or vCA1 (**H**) expressing jRCaMP7b (green) and the optical fiber (dotted yellow pane) implanted in the RE (top), and the electrode implanted in the MEC (bottom).

C, I Two examples showing synchronous recordings of Ca^{2+} activity of RE neurons projecting to mPFC (**C**, top) or vCA1 (**I**, top) and wavelet transforms of LFP in the MEC (**C** or **I**, bottom) during NREM sleep. Between two dotted white lines is theta frequency band (4-12 Hz).

D, J Heatmaps illustrating change of Ca^{2+} activity (top) and increment of theta/delta ratio (Δ Theta ratio, bottom) around the peak of Ca^{2+} activity of RE neurons projecting to mPFC (**D**) or vCA1 (**J**) during NREM sleep aligned to each animal ($n = 8$ mice).

E, K Average Ca^{2+} activity and Δ theta ratio around the peak of Ca^{2+} activity of RE neurons projecting to mPFC (**E**) or vCA1 (**K**) from 8 mice. Data are presented as mean (orange line) \pm SEM.

s.e.m. (shaded area), vertical dashed lines indicate the time points of Ca^{2+} peak.

F, L Statistic analysis of Δ theta ratio before and during the period of Ca^{2+} peak of RE neurons projecting to mPFC (**F**) or vCA1 (**L**). (Paired t test. mPFC: n = 8 mice, $t_7 = 0.456$, $P = 0.662$; vCA1: n = 7 mice, $t_6 = 1.021$, $P = 0.347$). Data are presented as mean \pm s.e.m..

Minor comments:

1. The author need to restructure the sentence in line 102-104 and clearly state the time period of behavioral studies for better understanding.

R: We have restructured the sentence as the follows (See line 99 on page 5) and clearly state the time period of behavioral studies.

“After six trials per day for consecutive three days of training during light phase (12:00 P.M.-18:00 P.M.), the animal gradually gained stable spatial memory, manifested as reaching the rewarded arm with a shorter path”.

2. Did the abbreviation PC stand for principal components or principal cells? Please indicate clearly when it first appeared in the line of 119.

R: We are sorry about that the abbreviation of PC was not clearly indicated. The abbreviation PC stand for principal components. We have indicated clearly when it first appeared (See line 112 on page 6).

3. Please explain the rationale for statistical methods in line 130-134 and provide reliable references.

4. Fig 1E: to provide the meaning of each element in the figure in legend, including capital letters A..D and different colors. In addition, please explain clearly the relationship between firing frequency/pattern, PC intensity and reactivation strength. Moreover, the author also needs to explain why the high reactivation values can reflect that the firing pattern is a closer match to learning-related firing pattern (line of 120-122).

R: Because all these two questions concern the reactivation of MEC neuronal assemble during NREM sleep, we reply these questions together as follows.

In fact, we analyzed reactivation of neuron firing patterns during NREM sleep according to the previous studies (Peyrache et al., Nature Neuroscience, 2009; Kim et al., Cell, 2019). This method uses principal components (PC) analysis to identify the firing patterns of neurons during learning. The outputs of this analysis are multiple PC, and the eigenvalue. High-rank PC, associated with larger eigenvalues (PC intensity) that exceeded the signal threshold defined as the theoretical upper bound of eigenvalues in the case of random spike trains, were referred to as signal PC components. After detecting the signal PC, then, we calculated the reactivation strength during post-training sleep, which represents “template matching” using the signal PC. High reactivation values indicate that the sleep firing patterns are a closer match to firing patterns detected during the learning.

We apologize for not providing a clear explanation of the rationale behind this method and failing to clearly indicate the relationship between firing pattern, PC intensity, and

reactivation strength. In the revised manuscript, we have thoroughly explained the rationale and clarified the relationship between firing pattern, PC intensity, and reactivation strength (*Refer to line 111-118 on page 6*). Additionally, we have included explanations for each element in Fig. 1E within the figure legend.

5. Fig 1F: the values of reactivation strength on day 1 and day 2 was about 1, but the firing pattern detected by principal component showed no reactivation cells in Fig 1E, please explain these contradictory results.

R: he method of calculating reactivation requires that each detected cell firing pattern includes all neurons rather than a subset. In our Fig. 1E, we mistakenly presented only a subset of recorded neurons as the firing pattern, which may give the impression that there are cells without reactivation. We apologize for this error and have corrected it by demonstrating that all cellular components exhibit reactivation during NREM sleep (*See Fig. 1E in the revised manuscript*).

6. Fig 1G upper: both raw signals and band-passed signals (0.5-4 Hz, 4-12 Hz) should be presented, same problem of Fig 2D.

Fig 1H-I: only theta events were analyzed, please complete the analysis of delta events.

Fig 1G-I: only LFP waves during NREM were shown, no signal of awakening stage was found.

Three points above are inconsistent with the result statement in the line of 146-148 'continuous delta waves (0.5-4 Hz) and discrete theta (4-12 Hz) events in the MEC recordings were evident during NREM sleep compared with that during the awakening stage'.

R: We revised these three issues according to your suggestions. In the Fig. 1G and Fig. 2D both raw signals and band-passed signals (0.5-4 Hz, 4-12 Hz) are presented. We showed the LFP waves of awakening stage (*See Extended Data Fig. 3A in the revised manuscript*). Furthermore, we have conducted an analysis of delta events during both wakefulness and sleep, and found that delta waves were most pronounced during NREM sleep, and its oscillation intensity was significantly higher than that during wakefulness. These newly analyzed results have been incorporated into the revised manuscript (*See Extended Data Fig. 3B and C in the revised manuscript*).

7. Fig 1I: the meaning of phrase 'Non-theta events' in the illustration is unclear. In addition, please check and correct the proportion value of theta band power and 'non-isolated theta' in the line of 151-152.

R: Indeed, the usage of phrase 'Non-theta events' in Fig. 1I is inappropriate. We meant to express the period during the non-isolated theta waves, but not the event itself. We corrected this issue and the phrase 'Non-theta events' has been revised to 'Non-isolated theta wave phase' (*See lines 151-153 on page 8*).

8. Extended Data Fig. 4: What's the meaning of 'integrated strength', and how to evaluate it.

R: We apologize for not providing a clear explanation of the term "integrated strength". In the initial version of the manuscript, integration strength was primarily defined as the area under the current curve during the stimulation period divided by the number of stimuli and duration of stimulation. While integrated strength represents the magnitude of currents per unit time during stimulation, it does not directly reflect the magnitude of excitatory postsynaptic currents (EPSCs) induced by stimuli with varying frequencies. Therefore, in our revised manuscript, we have calculated the mean amplitude of EPSCs induced by each stimulus to more accurately depict how MEC neurons respond to different frequency RE inputs. Under these conditions, when comparing 1 Hz and 20 Hz stimulations, we found that 5 Hz and 10 Hz still induce greater EPSCs, suggesting differential responses in MEC based on varying frequency stimulations (*See Extended Data Fig. 7B in the revised manuscript*).

9. The author needs to check the figures and legends thoroughly and complete the meaning of all elements in the figure legends.

R: Many thanks for you to point out this issue. The figures and legends have been thoroughly examined, and the meaning of all elements in the figure legends has been elucidated.

10. Please clearly indicate the number of animals used in the corresponding legend of each statistical chart.

R: We have clearly indicated the number of animals in each behavioral experiment in line with the reviewer's suggestion. The number of excluded animals and the sharing status of mice in each experiment are provided in detail in the figure legend.

In addition to the concerns raised by reviewer 1 (Major comment 1, Minor comments 3-6) regarding Figure 1, we have also taken into account the questions posed by other reviewers (Q3 from reviewer 2) concerning this figure. Consequently, significant modifications have been made to Figure 1 in light of the noteworthy phenomenon it depicts-reactivation accompanied by isolated theta oscillations during NREM sleep. These adjustments primarily include:

1) In Figure 1E of the original manuscript, we presented a firing pattern consisting of a subset of cells with high firing frequencies only, which led the reviewer to mistakenly assume that the reactivated neurons were predominantly interneurons. We have corrected this issue by showing that firing patterns and the corresponding all recorded neurons in the Fig. 1E.

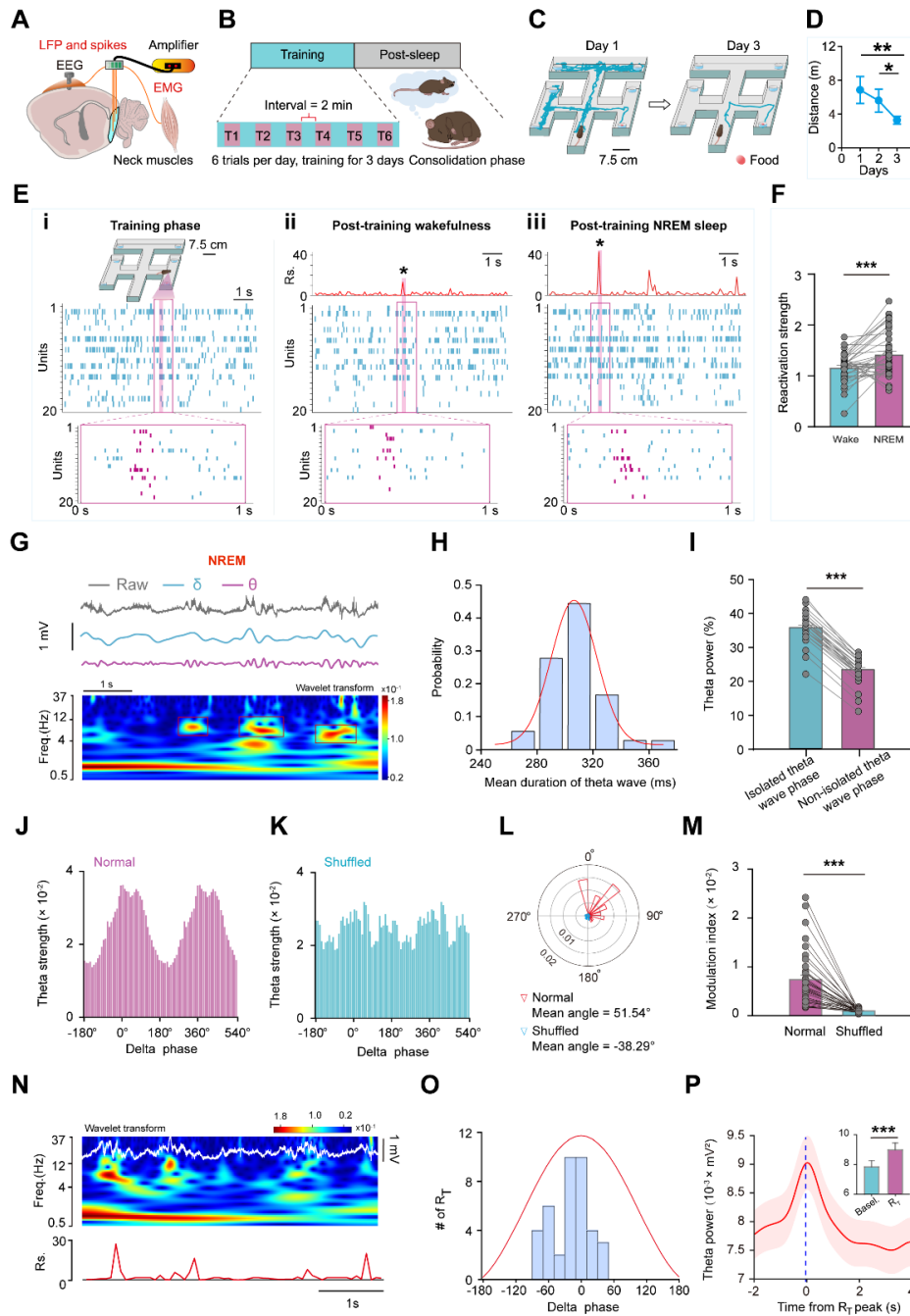
2) Presenting separate delta and theta oscillations after filtering the raw LFP in Fig. 1G, aiming to better illustrate that theta occurs during the upstates of delta oscillations.

3) Replacing the original distribution plot with a columnar statistical plot in Fig. 1I, for a more direct demonstration of high theta power during the isolated theta phase.

4) Substituting the schematic diagram in Fig. 1N with an improved version, which effectively highlights that reactivation consistently coincides with isolated theta waves during

NREM sleep.

The revised version of Figure 1 is also presented below (*Please refer to the Rfig. 10*).



Rfig. 10. Reactivation of medial entorhinal cortex (MEC) cells manifests isolated theta waves during non-rapid eye movement (NREM) sleep.

A Schematic diagram depicting LFP recording in the MEC and EEG-EMG recording.

B Experimental design of the spatial memory task. Training for 3 days, 6 trials per day.

C Representative trajectories of a mouse on the first day and the third day searching for food in the six-arm maze.

D The distance that animals traveled in the six-arm maze to acquire food each day (One-way RM ANOVA, $n = 6$ mice, $F_{2,5} = 7.079$, $P = 0.012$; day 1 vs. day 3, $P = 0.004$; day 1 vs. day 2, $P = 0.223$;

day 2 vs. day 3, $P = 0.037$). $**P < 0.01$, $*P < 0.05$.

Ei The representative MEC ensembles, comprising 20 cells, were recorded during the six-arm maze training phase with a magnified view (1 s) of a characteristic firing pattern (marked by purple color).

Eii Firing pattern of the same cells as (**Ei**), but during post-training wakefulness and with relatively low reactivation strength (R_s). The lower magnification shows the firing pattern corresponding to the peak of reactivation strength (black star) during post-training wakefulness.

Eiii Same as (**Eii**), but during post-training NREM sleep and with relatively high reactivation strength. The lower magnification shows the firing pattern corresponding to the peak of reactivation strength (black star) during post-training NREM sleep.

F Comparison of reactivation strength in the MEC ensembles during post-training NREM sleep and wakefulness (Paired t test, $n = 39$ channels from 6 mice, $t_{38} = -3.692$, $P < 0.001$). $***P < 0.001$.

G Representative raw trace of LFP recorded in the MEC (gray: raw trace; cyan: filtered delta; purple: filtered theta) and corresponding power spectrum during NREM sleep. Theta events detected is framed in the red rectangle box.

H Distributions of mean duration of the detected isolated theta waves during post-training NREM sleep. Red curve presents a normal distribution fit to this distribution. **I** Percentage of MEC LFP power in the theta band during detected isolated theta wave and non-isolated theta wave phases

(Wilcoxon Signed Rank Test, $n = 36$ channels from 6 mice, $Z = -5.243$, $P < 0.001$). $***P < 0.001$.

J, K Histograms showing the coupling strength of isolated theta waves and delta waves during NREM sleep for the normal (**J**) and shuffled data (**K**).

L Circular histogram of detected isolated theta waves relative to the delta phase in the normal group (red) and shuffled group (blue).

M Comparison of delta waves-theta waves coupling strength (modulation index) for the normal and shuffled data (Wilcoxon Signed Rank Test, $n = 36$ channels from 6 mice during post-training NREM sleep, $Z = -5.232$, $P < 0.001$). $***P < 0.001$.

N Representative raw trace of MEC LFP showing isolated theta waves and corresponding power spectrum, and reactivation strength (R_s) of MEC ensembles (bottom) during NREM sleep.

O Average distribution of reactivation events (R_T) during delta phase and a normal distribution fit to this distribution (red curve).

P Theta power around the peak of reactivation strength. Data are presented as mean (red line) \pm s.e.m. (shaded area). Inset in **P** is the comparison of theta power in the period of reactivation and baseline (Paired t -test, $n = 39$, $t_{38} = -8.998$, $P < 0.001$). $***P < 0.001$.

$N = 6$ mice were included in the experiment of recording spikes and LFP in the MEC.

One mouse was excluded due to inaccurate recording site. Data are presented as mean \pm s.e.m.

Reviewer #2 (Remarks to the Author):

Using a variety of cutting-edge technologies, such as single-unit electrophysiology, closed-loop optogenetics, Ca^{2+} photometry, and chemogenetics, Xiao et al. demonstrated that the medial entorhinal cortex (MEC) receives excitatory monosynaptic projections from the nucleus reuniens of the midline thalamus. Additionally, they discovered that the nucleus reuniens drives transient delta wave-nested theta events in the MEC during NREM sleep, facilitating memory reactivation following a spatial memory task and essential for memory consolidation.

This study presents a well-controlled investigation with intriguing and pioneering findings. Notably, besides the previously documented sharp waves, ripples, and spindles, this research unveils a new type of network oscillatory dynamics that instigate memory trace replay during sleep, shedding light on the associated neural circuit mechanisms. However, some points require attention in a revision to support the interpretation of results:

R: We appreciate the reviewer's positive evaluation of our work, as well as the valuable comments for the manuscript. All of your questions were answered one by one as follows.

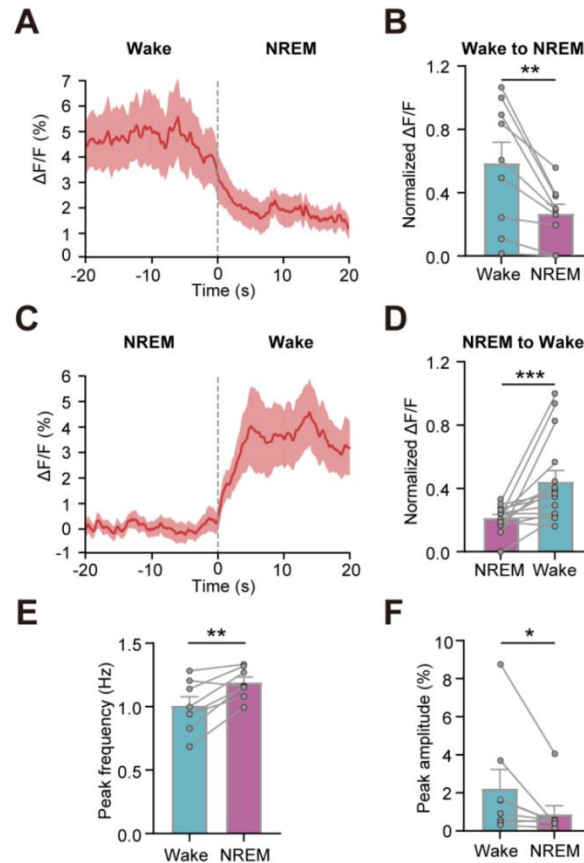
1. In Figures 2F and 2H, the authors demonstrated the existence of excitatory monosynaptic connections between RE and MEC through patch clamp recording combined with optogenetic techniques. However, the electrophysiological data primarily supported the conclusion through the application of glutamate receptor blockers, which may not be sufficient. It is recommended that the authors further analyze the latency of postsynaptic responses after optogenetic activation of the axonal terminals.

R: We appreciate reviewer for this valuable suggestion. We have further analyzed the latency of postsynaptic responses evoked by optogenetic stimulation of the axonal terminals. For both excitatory neurons and inhibitory neurons, we found latency of only around 5.45 ± 0.23 ms and 5.19 ± 0.31 ms, respectively. According to the report in the previous study (Ren et al., Nature Communications, 2024), this short latency further indicated the monosynaptic functional connections between the RE and MEC. These new analysis results have been included in the revised manuscript (See Fig.3C, E in the revised manuscript).

2. Figure 3 presents simultaneous recordings of EEG, EMG, and calcium signals, yet the analysis only delves into the relationship between calcium peaks and MEC local field potentials during NREM sleep. Further elucidation is needed regarding the changes in neurons projected by RE to MEC during awakening and NREM sleep.

R: Many thanks for this constructive suggestion. We have further analyzed the changes in activity of RE neurons projecting to MEC during awakening state. We found that during wakefulness, the RE neurons projecting to MEC were activated at a higher level, reflecting by the strong calcium activity. High-amplitude calcium spikes were also observed in these neurons during wakefulness; however, their occurrence frequency is relatively low (Refer to Rfig. 11). Simultaneously, enhanced synchronized gamma network oscillatory activity was observed between RE and MEC during wakefulness, while theta oscillatory synchrony was significantly reduced (Refer to Rfig. 3).

Therefore, these novel analysis findings indicate that RE neurons projecting to MEC exhibit more heightened activation during wakefulness as compared to the NREM sleep. This functional activity may be potentially associated with the generation of MEC gamma oscillation during wakefulness. These new analyses have been incorporated into a revised manuscript (See Extended Data Fig. 8 in the revised manuscript).



Rfig. 11. The changes in the activity of the RE neurons projecting to MEC across sleep and wakefulness.

A, C Average calcium activity of RE neurons projecting to MEC during transitions from wakefulness to NREM sleep (**A**), NREM sleep to wakefulness (**C**). Data are presented as mean (red line) \pm s.e.m. (shaded area), vertical dashed lines indicate the time points of state transitions.

B, D Average calcium activity and statistical analysis of 20 s before and after state transitions. Data are presented as mean \pm s.e.m. (Wake to NREM: $n = 9$ trials from 8 mice, paired t test, $t_8 = 3.789$, $P = 0.0053$; NREM to wake: $n = 15$ trials from 8 mice, Wilcoxon Signed Rank Test, $W = 112$, $P < 0.001$) *** $P < 0.001$, ** $P < 0.01$.

E, F Statistic analysis of calcium peak frequency (**E**) and amplitude (**F**) of RE neurons projecting to MEC during wakefulness and NREM sleep for 40 minutes recording. Data are presented as mean \pm s.e.m. ($n = 8$ mice. Peak frequency: paired t test, $t_7 = 3.929$, $P = 0.0057$; peak amplitude: Wilcoxon Signed Rank Test, $Z = -2.100$, $P = 0.0391$).

3. The authors mentioned including only animals with accurate recording sites. However, the number of excluded animals in some experiments, such as Figures 1 and 3, is not detailed. Moreover, clarity is needed on whether the same animals were used in Figures 2A-E and SI Fig. 5. Detailed information should be provided on these experiments.

R: We apologize for the insufficient provision of detailed information. We thoroughly examined each animal experiment, meticulously reviewing the number of animals utilized in various experiments as well as the criteria and rationale for excluding any animals from

analysis. Consequently, we have compiled a comprehensive table that precisely summarizes both the final count of mice included in our statistical analyses and the corresponding number of excluded mice (*Refer to the Table. 2*).

Table 2. A summary for the number of animals in each behavioral experiment

Figure #	Experiment	Number of mice were included	Number of mice were excluded	Reasons for exclusion
Fig.1F to 1P	Neuronal firing and local field potentials (LFPs) recording in the MEC during and following behavioral training.	N = 6 mice	1	one mouse: inaccurate location of electrode.
Fig.2	Simultaneous recording of spikes and LFPs in the RE, and LFPs in the MEC.	N = 5 mice	0	
Fig.4E to 4G	Simultaneous recording of calcium activities of RE neurons projecting to MEC and LFPs in the MEC.	N = 8 mice	0	
Fig.5D to 5I	Chemogenetic inhibition of RE-MEC pathway after training spatial memory.	N(mCherry) = 8 mice N(hM4D) = 9 mice	2	hM4D group: two mice were not included because they exhibited stereotyped behavior.
Fig.6	Closed-loop optogenetic inhibition of RE-MEC pathway during post-training NREM sleep.	N(eYFP) = 9 mice N(ArchT) = 8 mice	2	ArchT group: two mice, one mouse for no virus expression was observed, the other one for inaccurate optical fiber placement.
Extended Data Fig.1-3	Neuronal firing and local field potentials (LFPs) recording in the MEC during and following behavioral training. (Shared the same mice as Fig.1)	N = 6 mice	1	one mouse: inaccurate location of electrode.
Extended Data Fig.4A-E	RV-dsRed mediated retrograde tracing upstream brain regions of MEC.	N = 5 mice	0	
Extended Data Fig.4F-H	Retrobeads mediated retrograde tracing of MEC.	N = 4 mice	0	
Extended Data Fig.4I-J	Anterograde tracing of neuronal fibers in the MEC	N = 3 mice	0	

Extended Data Fig.5-6	Simultaneous recording of spikes and LFPs in the RE, and LFPs in the MEC. (Shared the same mice as Fig.2)	N = 5 mice	0	
Extended Data Fig.8	Simultaneous recording of calcium activities of RE neurons projecting to MEC and LFPs in the MEC. (Shared the same mice as Fig.4)	N = 8 mice	0	
Extended Data Fig.9A-F	Simultaneous recording of calcium activities of RE neurons projecting to medial prefrontal cortex (mPFC) and LFPs in the MEC.	N = 8 mice	0	
Extended Data Fig.9G-L	Simultaneous recording of calcium activities of RE neurons projecting to vCA1 and LFPs in the MEC.	N = 7 mice	0	
Extended Data Fig.10	Simultaneous recording of spikes and LFPs in the RE, and LFPs in the MEC. (Shared the same mice as Fig.2)	N = 5 mice	0	
Extended Data Fig.12	Closed-loop optogenetic inhibition of RE-MEC pathway during post-training NREM sleep. (Shared the same mice as Fig.6)	N(eYFP) = 9 mice N(ArchT) = 8 mice	2	ArchT group: one mouse for no virus expression was observed, the other one for inaccurate optical fiber placement.
Extended Data Fig.13	Optogenetic inhibition of RE-PRL pathway during NREM sleep	N(eYFP) = 6 mice N(ArchT) = 7 mice	0	

We have included relevant information regarding the utilization of animals in the aforementioned table within the revised manuscript. The legend accompanying each experiment provides detailed statistics on the number of animals involved, both included and excluded, as well as their sharing status (*See the figure legends for each experiment*).

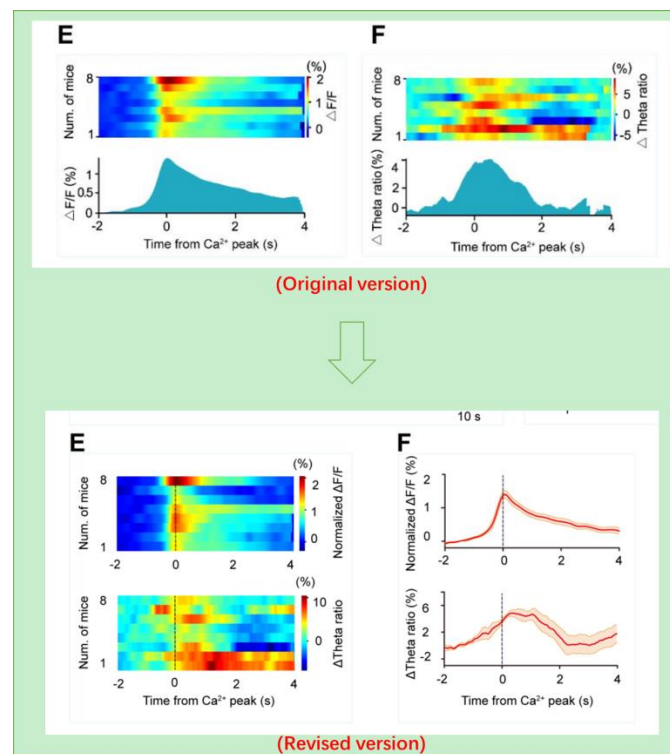
In addition to the revision of the figure legend, we have also taken into account the questions posed by other reviewers (Major comment 1, Minor comments 3-6) concerning Figure 1. Consequently, significant modifications have been made to Figure 1 (*Please refer to the Rfig. 10*).

4. The manuscript partially displays results in Figure 3, with vague descriptions.

Clarification is needed on how the data presented in Figures 3E and 3F.

R: We deeply appreciate the reviewer's suggestion. Indeed, we do not clearly describe the data presented in Figures 3E and 3F. In fact, for the Figure 3E, each line in the heat map represents the mean of the calcium peak value during NREM sleep for each animal. The line curve filled with blue color in the bottom represents the corresponding mean of the calcium signal for all mice ($n = 8$ mice). The Figure 3F illustrates the proportion of theta power corresponding to the calcium signal displayed in the Figure 3E. In the Figure 3F, each line in the heat map is the average percentage of theta power for each animal. The line curve filled with blue color in the bottom represents the average percentage of theta power for all mice. In the revised manuscript, we have detailed descriptions in the figure legends.

On the other hand, the way our data are presented is not straightforward enough. It mainly includes two aspects. First, our calcium signal and theta oscillations were collected synchronously, while the calcium signal and theta power were displayed separately in the Figure 3E and 3F. In order to solve this problem, we reorganized the Figures 3E and 3F, the calcium signal and theta power were stacked up and down, to synchronize display these two types of signals. Second, the line curve filled with blue color could only show the mean values of these calcium signal and theta power. Thus, it provided limited information. We have revised this issue by presenting this data using line plus error bar graph to show both the mean value and standard errors (*Refer to Rfig. 12*). The reorganized Figures 3E and 3F have been included in the revised manuscript (*See Fig. 4 E and F in the revised manuscript*).



Rfig. 12. The original and revised versions of the Figures 3E and 3F

5. Some statistical graphs appear non-uniformly presented, notably in Figure 5, differing from others. The authors should describe the statistical charts used and explain the rationale behind the varied presentation.

R: We thank the reviewer for pointing out this issue. We have checked all the statistical graphs in detail, and found that the statistical graphs are indeed non-uniformly presented, because the Figures 5F and 5G were presented with box plots, differing from others. The reason why we chose box plots for Figures 5F and 5G was based on the previous study (*Giri et al., Nature, 2024*), that is, if the data do not normally distribute, it is more appropriate to use this box plot to show the median and interquartile range. In Figures 5F and 5G, as the data about the reactivation strength in a eYFP and ArchT does not conform to the normal analysis, therefore, it would be more appropriate to utilize a box plot.

We sincerely apologize for the lack of description regarding the type of statistical graph presented in Figures 5F and 5G, as well as the reason behind our choice. This omission has led to a question from the reviewer. In response to this issue, we have clearly indicated the type of statistical graph and explain the reasons why we chose box plots for Figures 5F and 5G in the related figure legend (*See the figure legends of the Fig. 6F and 6G*).

Minor:

Figures 3 and Extended Data Fig. 6 depict optical fiber diagrams inconsistently. It is advisable to optimize and standardize these diagrams in the manuscript.

Some references lack standardized formats, urging further uniformity and standardization.

R: We have corrected these minor issues in line with reviewer's suggestions. In the Figures 3 and Extended Data Fig. 6, we have depicted optical fiber diagrams consistently. Furthermore, we have standardized the formats of all the references.

Reviewer #3 (Remarks to the Author):

The study conducted by Xiao et al. revealed that neural ensembles in the medial entorhinal cortex (MEC) responsible for encoding spatial experiences exhibit transient reactivation during NREM sleep, coinciding with isolated theta waves. Additionally, the authors observed that the nucleus reuniens (RE) in the midline thalamus demonstrates typical theta wave activity during NREM sleep, which is highly synchronized with the theta waves in the MEC. Through the application of a closed-loop optogenetic manipulation technique, the authors effectively inhibited the RE-MEC pathway, thereby suppressing isolated theta waves. This intervention led to impaired reactivation and compromised memory consolidation following a spatial memory task. These findings indicate that theta waves originating from the ventral midline thalamus play a crucial role in initiating memory reactivation. The manuscript is well-written, the figures are clearly presented, and the data support the conclusions. Knowledge gained from this study provides new information on

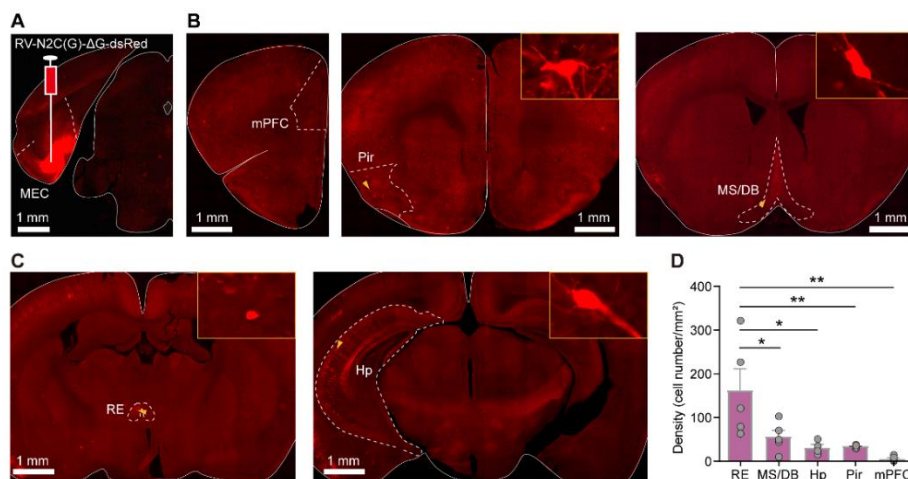
the role of the midline thalamus in regulating memory consolidation. A few minor points listed below need to be further addressed.

R: We appreciate the reviewer's the valuable comments and suggestions for the manuscript. The questions were answered one by one as follows.

1. For extended data fig2D, the data presented are the cell numbers in different brain regions. The authors should measure the size of each region and calculate the density of dsRed-labeled cells.

R: We are grateful for the suggestion. According to the reviewer's suggestion, we have measured the size of each brain region and enumerated the dsRed-labeled cells within these areas. The dimensions of nucleus reuniens (RE), medial septum/digonal band (MS/DB), piriform cortex (Pir), medial prefrontal cortex (mPFC), and hippocampus (Hp) were measured as 0.19 mm², 0.81 mm², 1.01 mm², 1.02 mm², and 4.6 mm² respectively. The average count of dsRed-labeled cells in RE, MS/DB, Pir, mPFC and Hp was 31, 45, 34, 6, and 138 correspondingly. Despite a higher number of neurons projecting to MEC in the Hp compared to RE; it is noteworthy that RE itself is significantly smaller in terms of size. Under these circumstances, we observed that the density of dsRed-labeled cells in RE reached its peak level surpassing other brain regions including Pir, Hp, MS/DB, and mPFC (Refer to Rfig. 13).

This new analysis result has been included in the revised manuscript (See Extended Data Fig. 4 in the revised manuscript).



Rfig. 13. MEC receives dense projections from the nucleus reuniens (RE).

A Example coronal section showing the viral injection center, as indicated by the expression of dsRed.

B Representative coronal sections showing the retrogradely labeled dsRed neurons. Inset, the enlarged view of a dsRed-positive neuron. mPFC: medial prefrontal cortex; Pir piriform cortex; MS/DB: Medial septum/digonal band.

C Same as C but for RE and hippocampus (Hp).

D Density of RV-labeled cells distributed in the brain regions identified as RE upstream areas.

Data are presented as mean \pm s.e.m. (One way ANOVA, $n = 5$ mice, $F_{4,19} = 6.599$, $P = 0.0017$). ****** $P < 0.01$, ***** $P < 0.05$.

2. In line 214, what is the exact duration of "a few milliseconds"? Please include the latency of light-evoked EPSC in excitatory and inhibitory neurons.

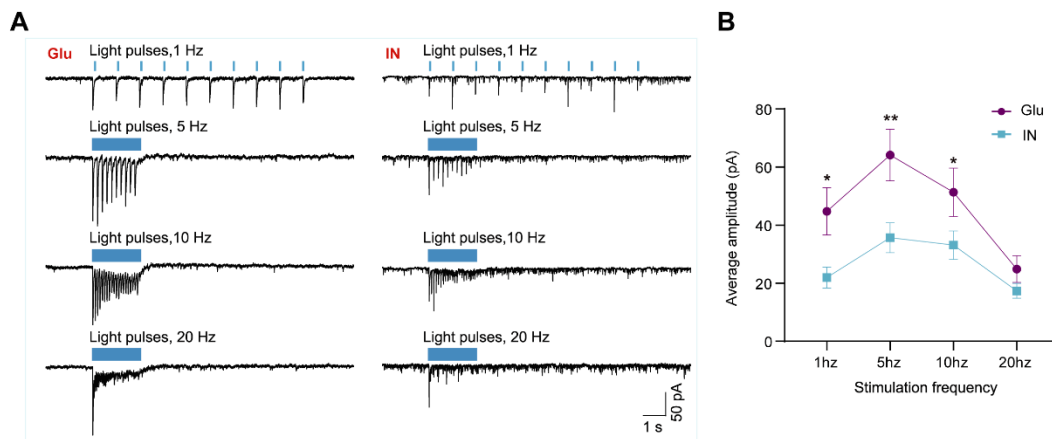
R: We are grateful to the reviewers for concerning this issue. The Q1 of reviewer 2 is also concerned about the exact duration of the latency. The detailed response to the Q1 of reviewer 2 has been provided for your reference. Here, we briefly reply this question again as follows.

We have further analyzed the latency of postsynaptic responses after optogenetic activation of the axonal terminals from the RE neurons. For the excitatory and inhibitory neurons, latencies were only around 5.45 ± 0.23 ms and 5.19 ± 0.31 ms, respectively. Based on the previous studies (*Ren et al., Nature Communications, 2024*), the short latency indicated the monosynaptic functions connections between the RE and MEC. These new analysis results have been included in the revised manuscript (*See Fig.3C, E in the revised manuscript*).

3. What are the oEPSC responses of interneurons to blue light stimulation at different frequencies? Please also include the sample traces next to extended data fig4B.

R: We deeply appreciate the reviewer's suggestion. We have further compared the EPSCs responses of interneurons to blue light stimulation at different frequencies. Our findings revealed that MEC interneurons exhibited greater response to 5 Hz and 10 Hz stimuli, whereas their response was weak for either 20 Hz stimuli. These results indicate the presence of frequency-dependent responses in interneurons (*Refer to Rfig. 14*). The revised manuscript now includes these additional analyses. Additionally, based on reviewer's suggestion, we included the sample traces of interneurons to the 1 Hz, 5 Hz, 10 Hz and 20 Hz stimuli (*See Extended Data Fig. 7 A and B in the revised manuscript*).

Of note, as the minor comment 8 of the reviewer 1 also concerns about how we calculated the integration strength for different stimuli, we briefly address this issue here. Integration strength was primarily defined as the area under the current curve during the stimulation period divided by the number of stimuli and duration of stimulation. While integrated strength could represent the magnitude of currents per unit time during stimulation, it does not directly reflect the MEC response to these varying frequencies. Therefore, in our revised manuscript, we have calculated the mean amplitude of EPSCs induced by each stimulus to more accurately depict how MEC neurons respond to different frequency RE inputs. Under these conditions, when comparing 1 Hz and 20 Hz stimulations, we found that 5 Hz and 10 Hz still induce greater EPSCs, suggesting differential responses in MEC based on varying frequency stimulations



Rfig. 14. The responses of excitatory neurons and interneurons to stimulation of RE inputs at different frequencies.

A Sample voltage-clamp traces showing excitatory postsynaptic currents (EPSCs) of a recorded glutamatergic neurons (left) or interneurons (right) evoked by a series of light pulses (1 Hz, 5 Hz, 10 Hz, 20 Hz).

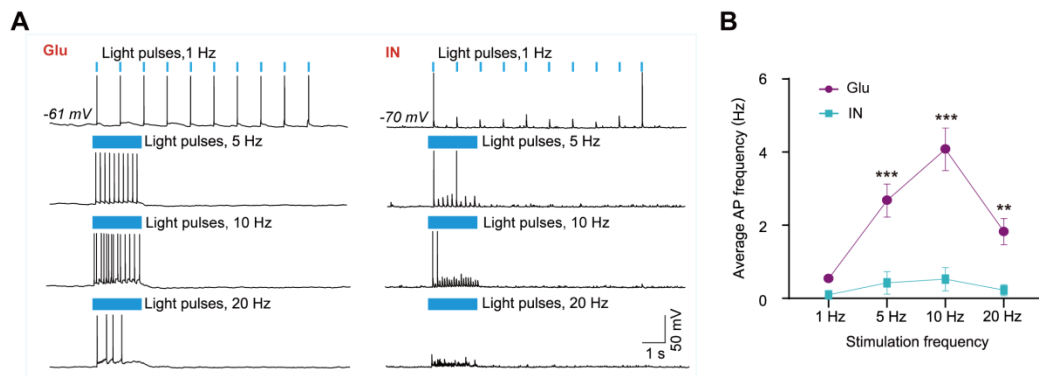
B Average amplitude of each EPSCs evoked by a series of light pulse (1 Hz, 5 Hz, 10 Hz, 20 Hz) of MEC glutamatergic neurons (purple) and GABAergic interneurons (cyan). (Two-way RM ANOVA, Glu: n = 13 cells, IN: n = 13 cells; Glu vs. IN, $F_{1,24} = 6.645$, $P = 0.018$; Light stimulation frequency factor, $F_{1,702, 40,85} = 24.67$, $P < 0.001$; interaction, $F_{3,72} = 3.18$, $P = 0.029$). ** $P < 0.01$, * $P < 0.05$.

4. What is the firing rate of excitatory neurons under basal conditions? Is 20 Hz stimulation considered too artificial, leading to a drop in the fidelity of light-evoked spikes after increasing the laser frequency?

R: We appreciate the reviewer to point out this issue. According to the previous study (Bozic et al., *Eur J Neurosci.* 2023), the average firing frequency of RE neurons during awake state is about 10 Hz. The firing frequency in about 15% of RE neurons can exceed 20 Hz. In addition, RE neurons can reliably respond to 20 Hz external stimulation, for example, 20 Hz optogenetic stimulation can induce discharge of RE neurons very stably (Goswamee et al., *Frontiers in Cellular Neuroscience*, 2021; Jayachandran et al., *Nature Communications*, 2023). Based on these previous studies, in our opinions, although under physiological conditions, the average firing frequency of RE neurons was below 20 Hz, RE neurons may have the ability to generate 20 Hz firing in response to optogenetic stimulation. The weakening of EPSC integration during 20 Hz stimulation may not be attributed to a decline in the fidelity of light-evoked spikes, but rather likely associated with the characteristics of postsynaptic MEC neurons.

5. Since fig2K shows the stimulation at 4 different frequencies, it would be appreciated to also include the sample traces of membrane voltage following 10 Hz light stimulation under the i-c mode.

R: The sample traces of membrane voltage following 1 Hz, 5 Hz, and 20 Hz stimulus were presented in the original version of our manuscript. However, we apologize for the absence of sample traces for 10 Hz light stimulation. According to the reviewer's suggestion, we have provided the sample traces of membrane voltage following 10 Hz light stimulation for both the excitatory neurons and interneurons (*Refer to Rfig. 15*). This issue has been revised accordingly in the revised manuscript (*See Fig.3 F and G in the revised manuscript*).



Rfig. 15. MEC neurons integrate monosynaptic excitatory inputs from the RE glutamatergic neurons in the theta band.

A Sample current-clamp traces showing responses evoked by light pulses of 1 Hz, 5 Hz, 10 Hz, 20 Hz of glutamatergic neurons (Glu, left) and GABAergic interneurons (IN, right) at resting state.

B Average frequency of active potentials evoked by light pulses (1 Hz, 5 Hz, 10 Hz, 20 Hz) of MEC glutamatergic neuron (purple, $n = 10$ cells) and GABAergic interneuron (cyan, $n = 10$ cells) (Two-way RMANOVA, Glu vs IN, $F_{1,18} = 24.30$, $P < 0.001$; light stimulation frequency factor, $F_{3,54} = 30.69$, $P < 0.001$; interaction, $F_{3,54} = 18.39$, $P < 0.001$). *** $P < 0.001$. ** $P < 0.01$.

6. Please include the averaged bars of amplitude for each group in fig2G and 2I. Line 231: "These results suggest that MEC excitatory glutamatergic neurons, rather than inhibitory interneurons, mainly integrate monosynaptic and excitatory inputs from RE at theta frequency band in vitro." This statement requires clarification, as depicted in fig2F-2K, where it is evident that over half of the interneurons in the MEC receive excitatory inputs from RE (with the averaged amplitude of oEPSCs appearing comparable between Glu and IN groups, and two cells exhibiting oEPSCs larger than 40 pA). Moreover, light stimulation resulted in action potentials following 5Hz stimulation, albeit with a low probability, indicating the potential involvement of a small subset of interneurons in the circuit function, possibly exerting a feed-forward inhibition on the excitatory glutamatergic neurons. Please revise the sentence accordingly.

7. Line 239: Instead of "high resting potential," use "hyperpolarized" for greater clarity.

8. Line 1220: The phrase "response to light pulses" may be confusing since no light is applied in the figure. Please rephrase this sentence to avoid confusion.

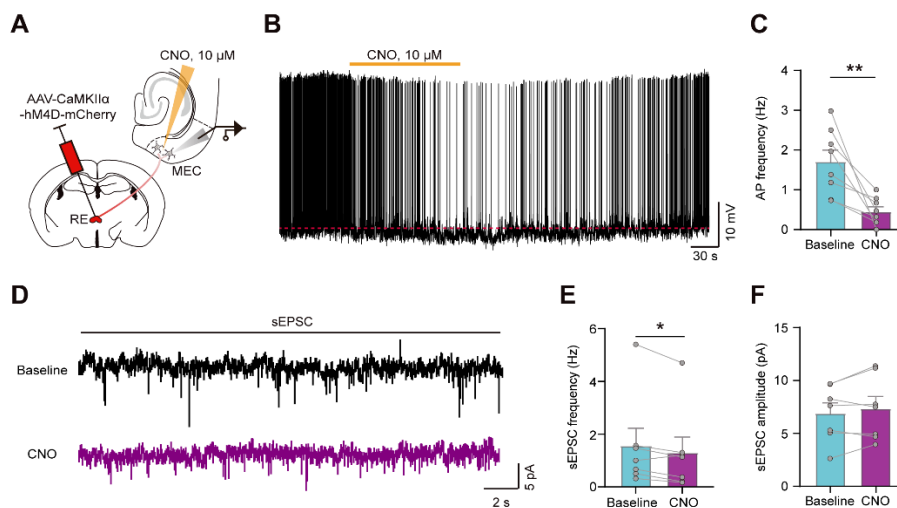
9. Line 1231: "recooded" should be corrected to "recorded."

10. Line 283: The text mentions CNO at 5 μM , but the label in fig4B is inconsistent. Please provide consistency between the text and the figure.

R: The Q6-Q10 are related to improper statements and presentation of the data, and we have corrected these issues according to the requirements of the reviewer.

11. Was the activity of cells in the MEC inhibited after bath application of CNO in the slice?

R: Thank you for your precious comments. We performed additional patch-clamp experiments to investigate the effects of CNO on neuronal activity in the MEC of mice expressing hM4D-mCherry in RE. Indeed, we observed a significant reduction in the firing frequency of MEC cells following administration of CNO in isolated brain slices. Moreover, CNO was found to selectively decrease the frequency of sEPECS while leaving the amplitude of sEPSCs unaffected (*Refer to Rfig. 16*). These findings further prove the effectiveness of the chemogenetic inhibition, which could effectively inhibit activity of MEC neurons. These new results have been included in the revised manuscript (*See Extended Data Fig. 11 in the revised manuscript*).



Rfig. 16. The activities of MEC excitatory neurons are down-regulated by chemogenetic inhibition of RE inputs.

A Schematic for recording the effect of CNO on the activities of MEC excitatory neurons receiving hM4D-expressed projections from RE.

B Sample traces showing activities of $\text{MEC}^{\text{RE-projecting}}$ neurons at the baseline and after bath application of CNO (10 μM , 2 min).

C Change of firing frequency of $\text{MEC}^{\text{RE-projecting}}$ neurons in a bath solution of CNO compared with baseline. (Paired t test, $n = 8$ cells, $t_7 = 3.812$, $P = 0.0066$).

D Representative traces of spontaneous excitatory postsynaptic currents (sEPSCs) of $\text{MEC}^{\text{RE-projecting}}$ neurons at the baseline and in a bath application of CNO.

E, F Statistic analysis of sEPSCs frequency (**E**) or amplitude (**F**) of $\text{MEC}^{\text{RE-projecting}}$ neurons at the baseline and in a bath application of CNO. (Paired t test. sEPSCs frequency: $n = 7$ cells, $t_6 = 2.625$,

$P = 0.0393$; sEPSCs amplitude: $n = 7$ cells, $t_6 = 1.133$, $P = 0.3003$). $*P < 0.05$.

12. Extended Data Fig6D demonstrates that delta power was increased in the ArchT group compared to eYFP mice. Could delta power also be related to memory regulation?

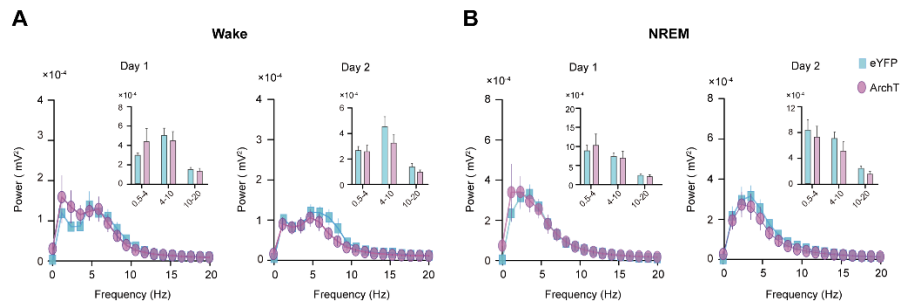
R: We thank the reviewer for pointing out this interesting question. In fact, the involvement of delta oscillations in the MEC in memory consolidation has not been previously reported. After reviewing the literature, it is generally considered that low-frequency oscillations, such as delta oscillations, primarily contribute to the restorative functions of sleep, including the removal of metabolic waste and the shrinkage of synaptic size to preserve morphological homeostasis (Tononi et al., Brain Res Bull. 2003; Fultz et al., Science, 2019). The more high-frequency oscillations nested in the delta waves, such as the delta-nested spindles (10-16 Hz) in the PFC, are more closely related to memory consolidation (Adamantidis et al., Nature Reviews Neuroscience, 2019).

Based on these previous studies, in our opinion, delta oscillations in the MEC may be closely associated with the homeostatic functions of NREM sleep; however, they may not serve as the primary oscillatory mechanism underlying memory consolidation. Nevertheless, it is important to note that this evidence remains indirect. In future research, selective manipulation of delta oscillations and subsequent observation of its impact on memory consolidation are warranted. According to the reviewer's suggestion, we have added the discussion for this issue (See lines 169-171 on page 9).

13. It would be appreciated if the power density analysis of NREM and REM sleep during post-training were included in Extended Data Fig6.

R: We carried out a new data analysis in line with reviewer's suggestion, we found that optogenetic inhibition of the RE-MEC pathway did not affect EEG power spectrum during awakening and NREM stage. These results further suggest that the impairment of memory consolidation was not an indirect effect caused by the change of sleep-wake (Refer to Rfig. 17). These new analysis results have been included in the revised manuscript (See Extended Data Fig. 12 H and I in the revised manuscript).

Of note, because we focused on the role of NREM sleep in memory consolidation, we only recorded wake-sleep states for only one hour of after training. Under this condition, it was found that REM sleep was only recorded in only 2 animals. Because REM sleep is recorded in fewer animals, therefore, we performed energy spectrum analysis mainly for wakefulness and NREM sleep, but not for REM sleep.



Rfig. 17. Closed-loop optogenetic inhibition of RE-MEC pathway did not affect EEG power spectrum during awakening and NREM stage.

A EEG power density of wakefulness during post-training 1 hour on day 1 and day 2. Inset in (H) is a quantitative analysis of the power in different frequency bands. Data are presented as mean \pm s.e.m.

B EEG power density of NREM sleep during post-training 1 hour on day 1 and day 2. Inset in (I) is a quantitative analysis of the power in different frequency bands. Data are presented as mean \pm s.e.m.

14. In fig5B, what do the black and blue/purple traces represent? Please add details to the legends.

R: We are sorry that we did not mark clearly to these traces. The blue and purple traces in fig5B represent the theta oscillatory activity after filtering raw local field potentials for the eYFP and ArchT groups, respectively. We have added the details to the related figure legends (*See figure legend of the Fig. 6B in the revised manuscript*).

15. For closed-loop Optogenetic Intervention, how do the authors avoid applying light to REM sleep, considering it also consists of theta power? Could you please add more details to the methods?

R: We are grateful to the reviewers for concerning this issue. The Q7 of reviewer 1 is also concerned about the question. We have given a detailed answer to the Q7 of reviewer 1 for your reference. Here, we would like to briefly address this question once again as follows.

The subject mouse was returned to the home cage immediately and the EEG-EMG recording was monitored to manually identify NREM episodes across the following 1 h. Once the mice entered NREM sleep, the laser generator was turned on, and the closed-loop system would specifically detect theta oscillations during NREM sleep to trigger the optogenetic stimulation. After quantification, 93.8% and 90.5% of the optogenetic stimulation were applied during NREM sleep for the ArchT group on day 1 and day 2, respectively. The very few other stimuli outside the NREM sleep fell during wakefulness, rather than REM sleep. These results suggest that intervention was selective under the NREM state. We have added this information in detail in the revised manuscript (*See lines 767-775 on page 42*).